EUROPEAN ORGANIZATION FOR NUCLEAR RESEARCH

LEP2FF/02-03

ALEPH 2002-039 PHYSIC 2002-015
DELPHI 2002-096 PHYS 926
L3 note 2785
OPAL TN727

7 October 2002

Combination of the LEP II $f\bar{f}$ Results

LEPEWWG $f\bar{f}$ Subgroup

Members :

C. Geweniger, C. Goy, M-N Minard
M. Elsing, J. Holt, W. Liebig, P. Renton
D. Bourilkov, S. Riemann, S. Wynhoff
K. Sachs, P. Ward

Abstract

Preliminary combinations of measurements of the 4 LEP collaborations of the process $e^+e^- \to f\bar{f}$ at LEP-II are presented, using data from the full LEP-II data set where available. Cross-sections and forward-backward asymmetry measurements are combined for the full LEP-II data set. Combined differential cross-sections $\frac{d\sigma}{d\cos\theta}$ for electron-pairs, muon-pair and tau-pair final states are presented. Measurements of the production of heavy flavours are combined. The combined results are interpreted in terms of contact interactions and the exchange of Z' bosons and leptoquarks, and within models of low scale gravity in large extra dimensions.

Results Prepared for Summer Conferences 2002

1 Introduction

During the LEP-II program LEP delivered collisions at energies from ~ 130 GeV to ~ 209 GeV. The 4 LEP experiments have made measurements on the $e^+e^- \to f\overline{f}$ process over this range of energies, and a preliminary combination of these data is discussed in this note.

In the years 1995 through 1999 LEP delivered luminosity at a number of distinct centre-of-mass energy points. In 2000 most of the luminosity was delivered close to 2 distinct energies, but there was also a significant fraction of the luminosity delivered in, more-or-less, a continuum of energies. To facilitate the combination of the data, the 4 LEP experiments all divided the data they collected in 2000 into two energy bins: from 202.5 to 205.5 GeV; and 205.5 GeV and above. The nominal and actual centre-of-mass energies to which the LEP data are averaged for each year are given in Table 1.

A number of measurements on the process $e^+e^- \to f\overline{f}$ exist and are combined. The preliminary averages of cross-section and forward-backward asymmetry measurements are discussed in Section 2. The results presented in this section update those presented in [1–5]. Complete results of the combinations are available on the web page [6]. In Section 3 a preliminary average of the differential cross-sections measurements, $\frac{d\sigma}{d\cos\theta}$, for the channels $e^+e^- \to e^+e^-$, $e^+e^- \to \mu^+\mu^-$ and $e^+e^- \to \tau^+\tau^-$ is presented. In Section 4 a preliminary combination of the heavy flavour results R_b, R_c, $A_{FB}^{b\overline{b}}$ and $A_{FB}^{c\overline{c}}$ from LEP-II is presented. In Section 5 the combined results are interpreted in terms of contact interactions and the exchange of Z′ bosons, the exchange of leptoquarks or squarks and the exchange of gravitons in large extra dimensions. The results are summarised in section 6.

There are significant changes with respect to results presented in Summer 2001 [1]:

- Changes to the combinations of results
  - updated preliminary cross-sections and leptonic forward-backward asymmetries for ALEPH
  - a new combination of preliminary differential cross-sections for e^+e^- final states
  - updated preliminary differential cross-section results for $\mu^+\mu^-$ and $\tau^+\tau^-$ final states from ALEPH
  - new preliminary heavy flavour results. Results are now averaged separately for $b\overline{b}$ and $c\overline{c}$ final states
- Changes to the interpretations of the combined results
  - previous results have been updated using the updated combinations
  - new interpretations of the updated data in terms of the exchange of leptoquarks
  - new interpretations of the e^+e^- final states in terms of contact interactions.

2 Averages for Cross-sections and Asymmetries

In this section the results of the preliminary combination of cross-sections and asymmetries are given. The individual experiments' analyses of cross-sections and forward-backward asymmetries are discussed in [7].

Cross-section results are combined for the $e^+e^- \to q\overline{q}$, $e^+e^- \to \mu^+\mu^-$ and $e^+e^- \to \tau^+\tau^-$ channels, forward-backward asymmetry measurements are combined for the $\mu^+\mu^-$ and $\tau^+\tau^-$

Year	Nominal Energy GeV	Actual Energy GeV	Luminosity pb^{-1}
1995	130	130.2	~ 3
	136	136.2	~ 3
	133*	133.2	~ 6
1996	161	161.3	~ 10
	172	172.1	~ 10
	167*	166.6	~ 20
1997	130	130.2	~ 2
	136	136.2	~ 2
	183	182.7	~ 50
1998	189	188.6	~ 170
1999	192	191.6	~ 30
	196	195.5	~ 80
	200	199.5	~ 80
	202	201.6	~ 40
2000	205	204.9	~ 80
	207	206.7	~ 140

Table 1: The nominal and actual centre-of-mass energies for data collected during LEP-II operation in each year. The approximate average luminosity analysed per experiment at each energy is also shown. Values marked with a * are average energies for 1995 and 1996 used for heavy flavour results. The data taken at nominal energies of 130 GeV and 136 GeV in 1995 and 1997 are combined by most experiments.

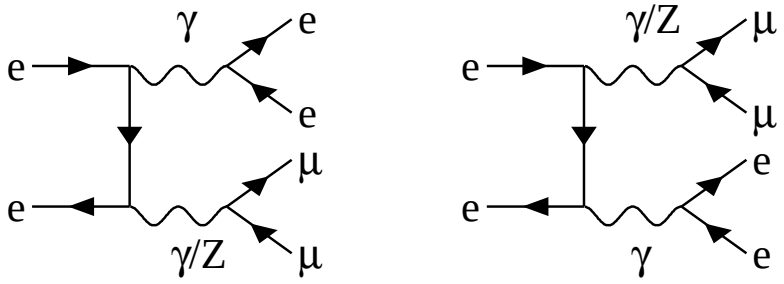

Figure 1: Diagrams leading to the the production of initial state non-singlet electron-positron pairs in $e^+e^- \to \mu^+\mu^-$, which are considered as signal in the common signal definition.

final states. The averages are made for the samples of events with high reduced centre-of-mass energies, $\sqrt{s'}$.

Individual experiments have their own $\mathrm{f\bar{f}}$ signal definitions; corrections are applied to bring the measurements to a common signal definitions:

- $\sqrt{s'}$ is taken to be the mass of the s-channel propagator, with the $\mathrm{f\bar{f}}$ signal being defined by the cut $\sqrt{s'/s} > 0.85$.
- ISR-FSR photon interference is subtracted to render the propagator mass unambiguous.
- Results are given for the full 4π angular acceptance.
- Initial state non-singlet diagrams, see for example Figure 1, which lead to events containing additional fermions pairs are considered as part of the two fermion signal. In such events, the additional fermion pairs are typically lost down the beampipe of the experiments, such that the visible event topologies are usually similar to a difermion events with photons radiated from the initial state.

The corrected measurement $\mathrm{M_{LEP}}$ is computed from the experimental measurement $\mathrm{M_{exp}}$,

$$\mathrm{M_{LEP}} = \mathrm{M_{exp}} + (\mathrm{P_{LEP}} - \mathrm{P_{exp}}),$$

where $\mathrm{P_{exp}}$ is the prediction for the measurement obtained for the experiments signal definition and $\mathrm{P_{LEP}}$ is the prediction for the common signal definition. The predictions are computed with ZFITTER [8].

In choosing a common signal definition there is a tension between the need to have a definition which is practical to implement in event generators and semi-analytical calculations, one which comes close to describing the underlying hard processes and one which most closely matches what is actually measured in experiments. Different signal definitions represent different balances between these needs. To illustrate how different choices would effect the quoted results a second signal definition is studied by calculating different predictions using ZFITTER:

- For dilepton events, $\sqrt{s'}$ is taken to be the bare invariant mass of the outgoing difermion pair.
- For hadronic events, it is taken to be the mass of the s-channel propagator.
- In both cases, ISR-FSR photon interference is included and the signal is defined by the cut $\sqrt{s'/s} > 0.85$. When calculating the contribution to the hadronic cross-section due to ISR-FSR interference, since the propagator mass is ill-defined, it is replaced by the bare $\mathrm{q\bar{q}}$ mass.

The definition of the hadronic cross-section is close to that used to define the signal for the heavy quark measurements given in Section 4.

Theoretical uncertainties associated with the Standard Model predictions for each of the measurements are not included during the averaging procedure, but must be included when assessing the compatibility of the data with theoretical predictions. The theoretical uncertainties on the Standard Model predictions amount to 0.26% on $\sigma(\mathrm{q\bar{q}})$, 0.4% on $\sigma(\mu^+\mu^-)$ and $\sigma(\tau^+\tau^-)$ and 0.004 on the leptonic forward-backward asymmetries [9].

The average is performed using the best linear unbiased estimator technique (BLUE) [10], which is equivalent to a χ^2 minimisation. All data from nominal centre-of-mass energies of 130–207 GeV are averaged at the same time.

Particular care is taken to ensure that the correlations between the hadronic cross-sections are reasonably estimated. As in [1] the errors are broken down into 5 categories

1) The statistical uncertainty plus uncorrelated systematic uncertainties, combined in quadrature.

2) The systematic uncertainty for the final state X which is fully correlated between energy points for that experiment.

3) The systematic uncertainty for experiment Y which is fully correlated between different final states for this energy point.

4) The systematic uncertainty for the final state X which is fully correlated between energy points and between different experiments.

5) The systematic uncertainty which is fully correlated between energy points and between different experiments for all final states.

Uncertainties in the hadronic cross-sections arising from fragmentation models and modelling of ISR are treated as fully correlated between experiments. Despite some differences between the models used and the methods of evaluating the errors in the different experiments, there are significant common elements in the estimation of these sources of uncertainty.

New, preliminary, results from ALEPH are included in the average. The updated ALEPH measurements use a lower cut on the reduced centre-of-mass energy, which makes the signal definition of ALEPH closer to the combined LEP signal definition.

Table 2 gives the averaged cross-sections and forward-backward asymmetries for all energies. The differences in the results obtained when using predictions of ZIFFTER for the second signal definition are also given. The differences are significant when compared to the precision obtained from averaging together the measurments at all energies. The χ^2 per degree of freedom for the average of the LEP-II $\mathrm{f\bar{f}}$ data is 160/180. The correlations are rather small, with the largest components at any given pair of energies being between the hadronic cross-sections. The other off-diagonal terms in the correlation matrix are smaller than 10%. The correlation matrix between the averaged hadronic cross-sections at different centre-of-mass energies is given in Table 3. Differences in the results with respect to previous combinations at centre-of-mass energies from 130–207 GeV [1] arise from the updates to the ALEPH results.

Figures 2 and 3 show the LEP averaged cross-sections and asymmetries, respectively, as a function of the centre-of-mass energy, together with the SM predictions. There is good agreement between the SM expectations and the measurements of the individual experiments and the combined averages. The cross-sections for hadronic final states at most of the energy points are somewhat above the SM expectations. Taking into account the correlations between the data points and also taking into account the theoretical error on the SM predictions, the ratio of the measured cross-sections to the SM expectations, averaged over all energies, is approximately a 1.7 standard deviation excess. The correlations are significant and must be included when estimating the compatibility of the data with theoretical predictions, otherwise the significance of the excess is overestimated, if they are ignored the excess is calculated to be 2.8 standard deviations. It is concluded that there is no significant evidence in the results of the combinations for physics beyond the SM in the process $\mathrm{e^+e^-} \to \mathrm{f\bar{f}}$.

$\sqrt{s}$ (GeV)	Quantity	Average value	SM	Δ
130	$\sigma(q\overline{q})$ [pb]	82.062±2.227	82.803	-0.251
130	$\sigma(\mu^+\mu^-)$ [pb]	8.619±0.682	8.439	-0.331
130	$\sigma(\tau^+\tau^-)$ [pb]	9.024±0.930	8.435	-0.108
130	$A_{fb}(\mu^+\mu^-)$	0.694±0.060	0.705	0.012
130	$A_{fb}(\tau^+\tau^-)$	0.663±0.076	0.704	0.012
136	$\sigma(q\overline{q})$ [pb]	66.673±1.971	66.596	-0.224
136	$\sigma(\mu^+\mu^-)$ [pb]	8.273±0.677	7.281	-0.280
136	$\sigma(\tau^+\tau^-)$ [pb]	7.078±0.820	7.279	-0.091
136	$A_{fb}(\mu^+\mu^-)$	0.708±0.060	0.684	0.013
136	$A_{fb}(\tau^+\tau^-)$	0.753±0.088	0.683	0.014
161	$\sigma(q\overline{q})$ [pb]	36.979±1.071	35.247	-0.143
161	$\sigma(\mu^+\mu^-)$ [pb]	4.608±0.363	4.613	-0.178
161	$\sigma(\tau^+\tau^-)$ [pb]	5.667±0.544	4.613	-0.061
161	$A_{fb}(\mu^+\mu^-)$	0.538±0.067	0.609	0.017
161	$A_{fb}(\tau^+\tau^-)$	0.646±0.077	0.609	0.016
172	$\sigma(q\overline{q})$ [pb]	29.233±0.986	28.738	-0.124
172	$\sigma(\mu^+\mu^-)$ [pb]	3.572±0.317	3.952	-0.157
172	$\sigma(\tau^+\tau^-)$ [pb]	4.010±0.449	3.951	-0.054
172	$A_{fb}(\mu^+\mu^-)$	0.675±0.077	0.591	0.018
172	$A_{fb}(\tau^+\tau^-)$	0.342±0.094	0.591	0.017
183	$\sigma(q\overline{q})$ [pb]	24.592±0.423	24.200	-0.109
183	$\sigma(\mu^+\mu^-)$ [pb]	3.492±0.147	3.446	-0.139
183	$\sigma(\tau^+\tau^-)$ [pb]	3.370±0.174	3.446	-0.050
183	$A_{fb}(\mu^+\mu^-)$	0.559±0.035	0.576	0.018
183	$A_{fb}(\tau^+\tau^-)$	0.608±0.045	0.576	0.018
189	$\sigma(q\overline{q})$ [pb]	22.472±0.246	22.156	-0.101
189	$\sigma(\mu^+\mu^-)$ [pb]	3.123±0.076	3.207	-0.131
189	$\sigma(\tau^+\tau^-)$ [pb]	3.195±0.104	3.207	-0.048
189	$A_{fb}(\mu^+\mu^-)$	0.569±0.021	0.569	0.019
189	$A_{fb}(\tau^+\tau^-)$	0.596±0.026	0.569	0.018
192	$\sigma(q\overline{q})$ [pb]	22.052±0.528	21.237	-0.098
192	$\sigma(\mu^+\mu^-)$ [pb]	2.920±0.179	3.097	-0.127
192	$\sigma(\tau^+\tau^-)$ [pb]	2.811±0.227	3.097	-0.047
192	$A_{fb}(\mu^+\mu^-)$	0.553±0.051	0.566	0.019
192	$A_{fb}(\tau^+\tau^-)$	0.615±0.069	0.566	0.019
196	$\sigma(q\overline{q})$ [pb]	20.527±0.340	20.127	-0.094
196	$\sigma(\mu^+\mu^-)$ [pb]	2.945±0.108	2.962	-0.123
196	$\sigma(\tau^+\tau^-)$ [pb]	2.936±0.144	2.962	-0.045
196	$A_{fb}(\mu^+\mu^-)$	0.581±0.031	0.562	0.019
196	$A_{fb}(\tau^+\tau^-)$	0.505±0.044	0.562	0.019
200	$\sigma(q\overline{q})$ [pb]	19.249±0.317	19.085	-0.090
200	$\sigma(\mu^+\mu^-)$ [pb]	3.016±0.107	2.834	-0.118
200	$\sigma(\tau^+\tau^-)$ [pb]	2.895±0.139	2.833	-0.044
200	$A_{fb}(\mu^+\mu^-)$	0.524±0.031	0.558	0.019
200	$A_{fb}(\tau^+\tau^-)$	0.539±0.042	0.558	0.019
202	$\sigma(q\overline{q})$ [pb]	19.071±0.436	18.572	-0.088
202	$\sigma(\mu^+\mu^-)$ [pb]	2.583±0.141	2.770	-0.116
202	$\sigma(\tau^+\tau^-)$ [pb]	2.788±0.195	2.769	-0.044
202	$A_{fb}(\mu^+\mu^-)$	0.547±0.047	0.556	0.020
202	$A_{fb}(\tau^+\tau^-)$	0.589±0.059	0.556	0.019
205	$\sigma(q\overline{q})$ [pb]	18.171±0.313	17.811	-0.085
205	$\sigma(\mu^+\mu^-)$ [pb]	2.449±0.100	2.674	-0.112
205	$\sigma(\tau^+\tau^-)$ [pb]	2.777±0.139	2.673	-0.042
205	$A_{fb}(\mu^+\mu^-)$	0.565±0.035	0.553	0.020
205	$A_{fb}(\tau^+\tau^-)$	0.571±0.042	0.553	0.019
207	$\sigma(q\overline{q})$ [pb]	17.492±0.256	17.418	-0.083
207	$\sigma(\mu^+\mu^-)$ [pb]	2.595±0.088	2.623	-0.111
207	$\sigma(\tau^+\tau^-)$ [pb]	2.530±0.106	2.623	-0.042
207	$A_{fb}(\mu^+\mu^-)$	0.542±0.027	0.552	0.020
207	$A_{fb}(\tau^+\tau^-)$	0.564±0.037	0.551	0.019

Table 2: Preliminary combined LEP results for $e^+e^- \to f\bar{f}$. All the results correspond to the signal first signal definition given in the text. The Standard Model predictions are from ZFITTER [8]. The difference, Δ, in the predictions of ZFITTER for second definition relative to the first are given in the final column. The quoted uncertainties do not include the theoretical uncertainties on the corrections discussed in the text.

Table 3: The correlation coefficients between averaged hadronic cross-sections at different energies.

$\sqrt{s}$ GeV)	130	136	161	172	183	189	192	196	200	202	205	207
130	1.000	0.071	0.080	0.072	0.114	0.146	0.077	0.105	0.120	0.086	0.117	0.138
136	0.071	1.000	0.075	0.067	0.106	0.135	0.071	0.097	0.110	0.079	0.109	0.128
161	0.080	0.075	1.000	0.077	0.120	0.153	0.080	0.110	0.125	0.090	0.124	0.145
172	0.072	0.067	0.077	1.000	0.108	0.137	0.072	0.099	0.112	0.081	0.111	0.130
183	0.114	0.106	0.120	0.108	1.000	0.223	0.117	0.158	0.182	0.129	0.176	0.208
189	0.146	0.135	0.153	0.137	0.223	1.000	0.151	0.206	0.235	0.168	0.226	0.268
192	0.077	0.071	0.080	0.072	0.117	0.151	1.000	0.109	0.126	0.090	0.118	0.138
196	0.105	0.097	0.110	0.099	0.158	0.206	0.109	1.000	0.169	0.122	0.162	0.190
200	0.120	0.110	0.125	0.112	0.182	0.235	0.126	0.169	1.000	0.140	0.184	0.215
202	0.086	0.079	0.090	0.081	0.129	0.168	0.090	0.122	0.140	1.000	0.132	0.153
205	0.117	0.109	0.124	0.111	0.176	0.226	0.118	0.162	0.184	0.132	1.000	0.213
207	0.138	0.128	0.145	0.130	0.208	0.268	0.138	0.190	0.215	0.153	0.213	1.000

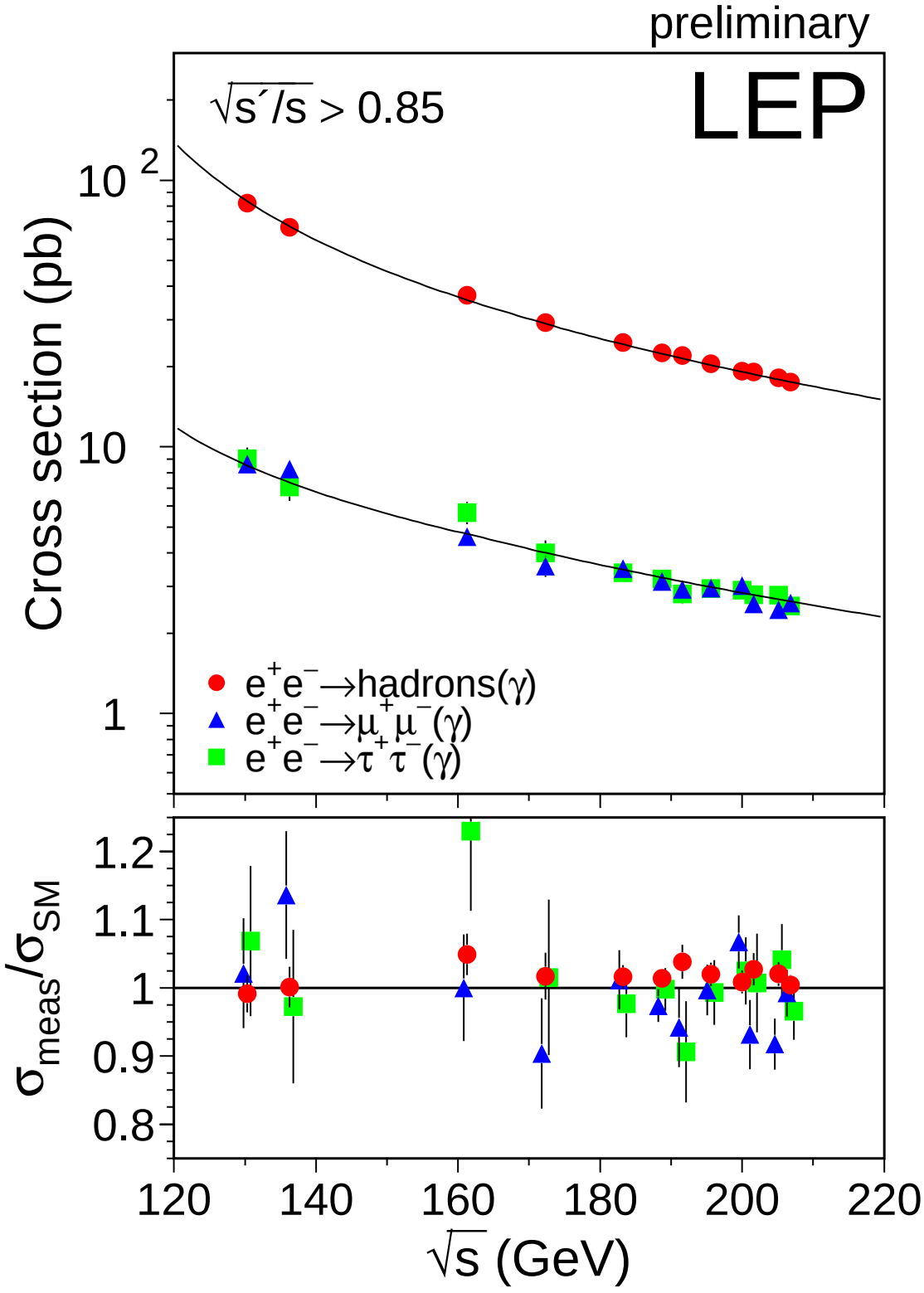

Figure 2: Preliminary combined LEP results on the cross-sections for $q\overline{q}$, $\mu^+\mu^-$ and $\tau^+\tau^-$ final states, as a function of centre-of-mass energy. The expectations of the SM, computed with ZFITTER [8], are shown as curves. The lower plot shows the ratio of the data divided by the SM.

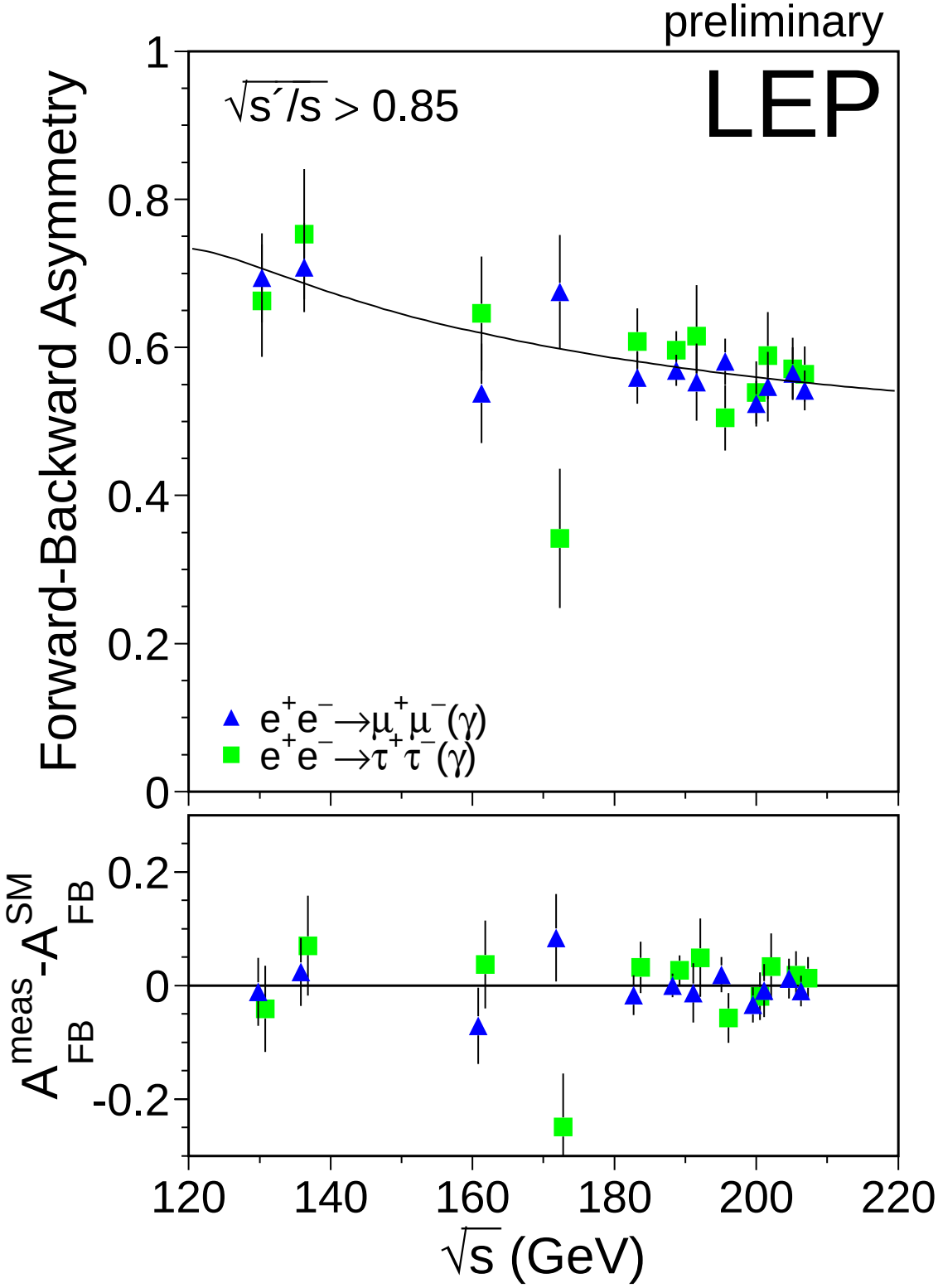

Figure 3: Preliminary combined LEP results on the forward-backward asymmetry for $\mu^+\mu^-$ and $\tau^+\tau^-$ final states as a function of centre-of-mass energy. The expectations of the SM computed with ZFITTER [8], are shown as curves. The lower plot shows differences between the data and the SM.

3 Averages for Differential Cross-sections

3.1 e^+e^- final states

The LEP experiments have measured the differential cross-section, $\frac{d\sigma}{d\cos\theta}$, for the $e^+e^- \to e^+e^-$ channel for samples of events. cA preliminary combination of these results is made by performing a χ^2 fit to the measured differential cross-sections, using the statistical errors as given by the experiments. In contrast to the muon and tau channels (Section 3.2) the higher statistics makes the use of expected statistical errors unnecessary.

The combination includes data from 189 GeV to 207 GeV, but not all experiments provide data at these energies. The data used in the combination are summarised in Table 4.

Each experiment's data are binned according to an agreed common definition, which takes into account the large forward peak of Bhabha scattering:

- 10 bins for $\cos\theta$ between 0.0 and 0.90 and
- 5 bins for $\cos\theta$ between -0.90 and 0.0

at each energy. The scattering angle, θ, is the angle of the negative lepton with respect to the incoming electron direction in the lab coordinate system. The outer acceptances of the most forward and most backward bins for which the experiments present their data are different. The ranges in $\cos\theta$ of the individual experiments and the average are given in Table 5. Except for the binning, each experiment uses their own signal definition, for example different experiments have different acollinearity cuts to select events. The signal definition used for the LEP average corresponds to an acollinearity cut of 10°. The experimental measurements are corrected to the common signal definition following the procedure described in Section 2. The theoretical predictions are taken from the Monte Carlo event generator BHWIDE [11].

Correlated systematic errors between different experiments, energies and bins at the same energy, arising from uncertainties on the overall normalisation, and from migration of events between forward and backward bins with the same absolute value of $\cos\theta$ due to uncertainties in the corrections for charge confusion, were considered in the averaging procedure.

An average for all energies between 189–207 GeV is performed. The results of the averages are shown in Figure 4. The χ^2 per degree of freedom for the average is 190.8/189.

The correlations between bins in the average are well below 5% of the total error on the averages in each bin for most of the cases, and exceed 10% for the most forward bin for the energy points with the highest accumulated statistics. The agreement between the averaged data and the predictions from the Monte Carlo generator BHWIDE is good.

3.2 $\mu^+\mu^-$and $\tau^+\tau^-$ final states

The LEP experiments have measured the differential cross-section, $\frac{d\sigma}{d\cos\theta}$, for the $e^+e^- \to \mu^+\mu^-$ and $e^+e^- \to \tau^+\tau^-$ channels for samples of events with $\sqrt{s'/s} > 0.85$. A preliminary combination of these results is made using the BLUE technique. The statistical error associated with each measurments is taken as the expected statistical error on the differential cross-sections, computed from the expected numbers of events in each bin for each experiment. Using a Monte Carlo simulation it has been shown that this method provides a good approximation to the exact likelihood method based on Poisson statistics [3].

	$e^+e^- \to e^+e^-$			
$\sqrt{s}$(GeV)	A	D	L	O
189	P	-	P	F
192–202	P	-	P	P
205–207	P	-	P	P

Table 4: Differential cross-section data provided by the LEP collaborations (ALEPH, DELPHI, L3 and OPAL) for $e^+e^- \to e^+e^-$. Data indicated with F are final, published data. Data marked with P are preliminary. Data marked with a - were not available for combination.

Experiment	$\cos\theta_{min}$	$\cos\theta_{max}$
ALEPH ($\sqrt{s'/s} > 0.85$)	-0.90	0.90
L3 (acol. $< 25°$)	-0.72	0.72
OPAL (acol. $< 10°$)	-0.90	0.90
Average (acol. $< 10°$)	-0.90	0.90

Table 5: The acceptances for which experimental data are presented for the $e^+e^- \to e^+e^-$ channel and the acceptance for the LEP average.

	$e^+e^- \to \mu^+\mu^-$				$e^+e^- \to \tau^+\tau^-$			
$\sqrt{s}$(GeV)	A	D	L	O	A	D	L	O
183	-	F	-	F	-	F	-	F
189	P	F	F	F	P	F	F	F
192–202	P	P	P	P	P	P	-	P
205–207	P	P	P	P	P	P	-	P

Table 6: Differential cross-section data provided by the LEP collaborations (ALEPH, DELPHI, L3 and OPAL) for $e^+e^- \to \mu^+\mu^-$ and $e^+e^- \to \tau^+\tau^-$ combination at different centre-of-mass energies. Data indicated with F are final, published data. Data marked with P are preliminary. Data marked with a - were not available for combination.

Experiment	$\cos\theta_{min}$	$\cos\theta_{max}$
ALEPH	-0.95	0.95
DELPHI ($e^+e^- \to \mu^+\mu^-$ 183)	-0.94	0.94
DELPHI ($e^+e^- \to \mu^+\mu^-$ 189–207)	-0.97	0.97
DELPHI ($e^+e^- \to \tau^+\tau^-$)	-0.96	0.96
L3	-0.90	0.90
OPAL	-1.00	1.00
Average	-1.00	1.00

Table 7: The acceptances for which experimental data are presented and the acceptance for the LEP average. For DELPHI the acceptance is shown for the different channels and for the muons for different centre of mass energies. For all other experiments the acceptance is the same for muon and tau-lepton channels and for all energies provided.

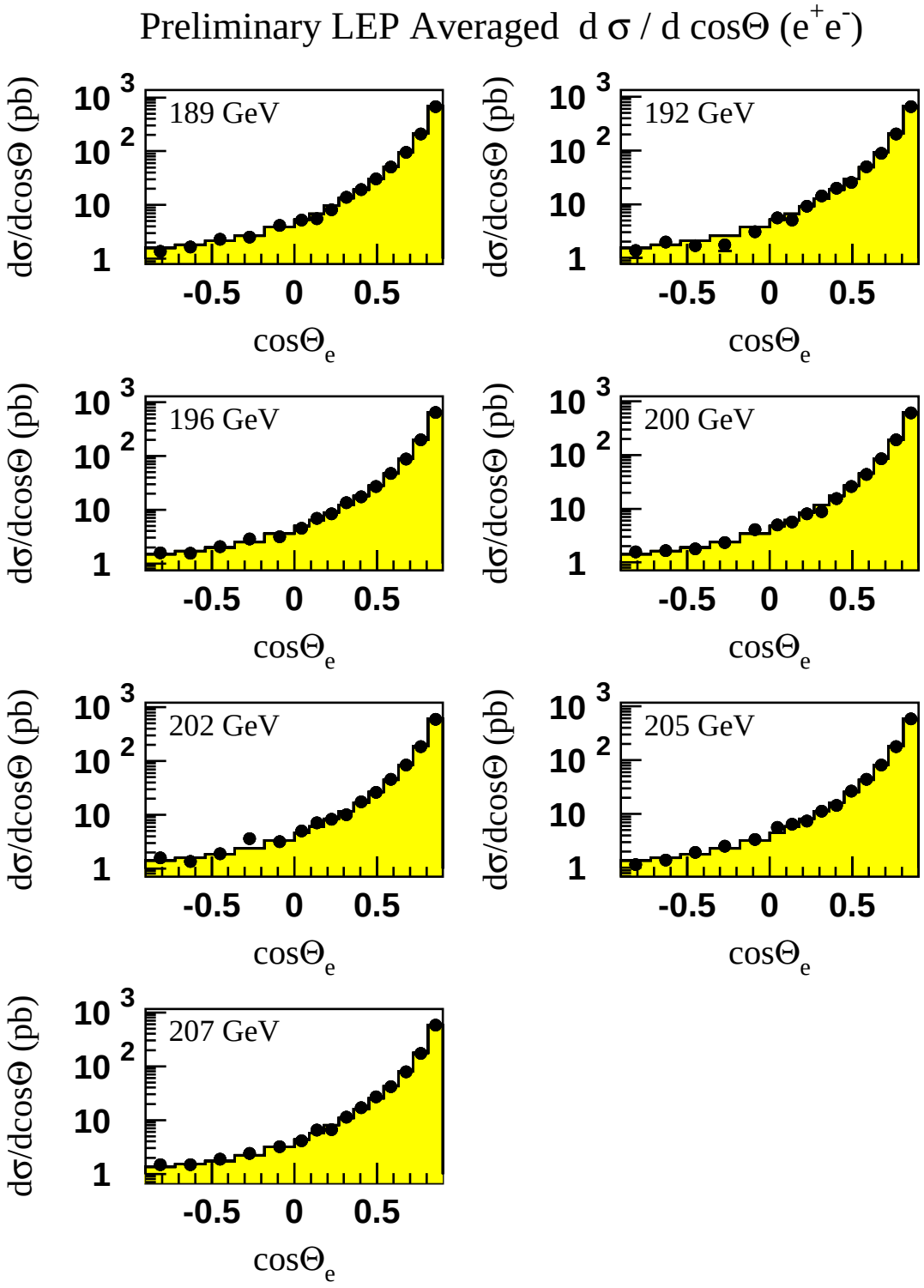

Figure 4: LEP averaged differential cross-sections for $e^+e^- \to e^+e^-$ at energies of 189–207 GeV. The SM predictions, shown as solid histograms, are computed with BHWIDE [11].

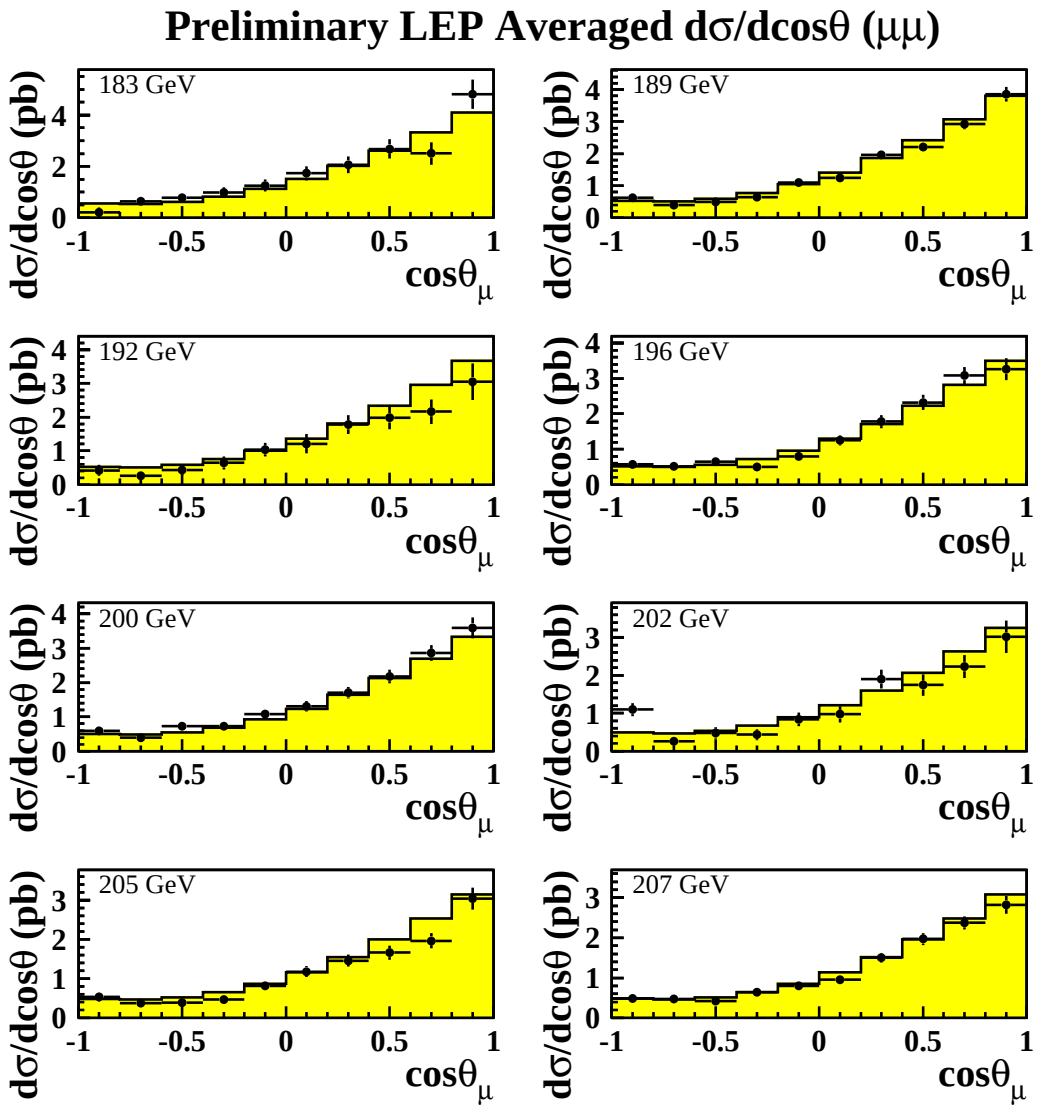

Figure 5: LEP averaged differential cross-sections for $e^+e^- \to \mu^+\mu^-$ at energies of 183–207 GeV. The SM predictions, shown as solid histograms, are computed with ZFITTER [8].

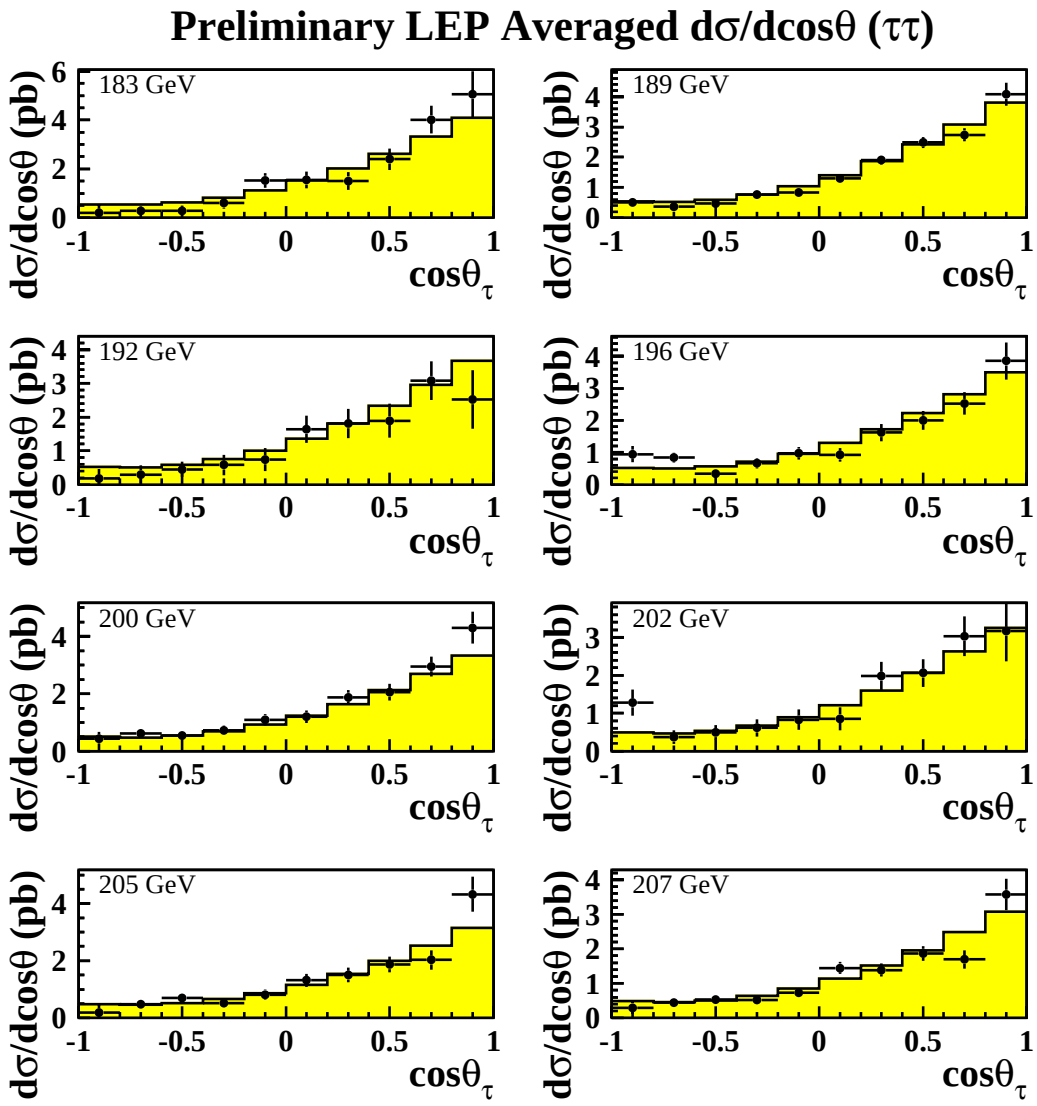

Figure 6: LEP averaged differential cross-sections for $e^+e^- \to \tau^+\tau^-$ at energies of 183–207 GeV. The SM predictions, shown as solid histograms, are computed with ZFITTER [8].

The combination included data from 183 GeV to 207 GeV, but not all experiments provided data at all energies. Since [1], the ALEPH results have been updated. The data used in the combination are summarised in Table 6.

Each experiment's data are binned in 10 bins of $\cos\theta$ at each energy, using their own signal definition. The scattering angle, θ, is the angle of the negative lepton with respect to the incoming electron direction in the lab coordinate system. The outer acceptances of the most forward and most backward bins for which the four experiments present their data are different. This was accounted for as part of the correction to a common signal definition. The ranges in $\cos\theta$ for the measurements of the individual experiments and the average are given in Table 7. The signal definition used corresponded to the first definition given in Section 2.

Correlated systematic errors between different experiments, channels and energies, arising from uncertainties on the overall normalisation are considered in the averaging procedure. Previously [1] three separate averages were performed for different centre-of-mass energies; one for 183 and 189 GeV data, one for 192–202 GeV data and for 205 and 207 GeV data, which resulted in missing correlations between measurements in different groups of energies. Now all data from all energies are combined in a single average

The results of the averages are shown in Figures 5 and 6. The correlations between bins in the average are less that 2% of the total error on the averages in each bin. Overall the agreement between the averaged data and the predictions is reasonable, with a χ^2 of 200 for 160 degrees of freedom. At 202 GeV the measured differential cross-sections in the most backward bins, $-1.00 < \cos\theta < 0.8$, for both muon and tau final states are above the predictions. The data at 202 GeV suffer from rather low delivered luminosity, with less than 4 events expected in each experiment in each channel in this backward $\cos\theta$ bin. The agreement between the data and the predictions in the same $\cos\theta$ bin is more consistent at higher energies.

4 Averages for Heavy Flavour Measurements

This section presents a preliminary combination of both published [12] and preliminary [13] measurements of the ratios* R_{b} and R_{c} and the forward-backward asymmetries, $A_{\mathrm{FB}}^{\mathrm{b\overline{b}}}$ and $A_{\mathrm{FB}}^{\mathrm{c\overline{c}}}$, from the LEP collaborations at centre-of-mass energies in the range of 130 GeV to 207 GeV. The averages have been updated with respect to [1]. New, preliminary, results from ALEPH on $A_{\mathrm{FB}}^{\mathrm{b\overline{b}}}$ at centre-of-mass energies of 205 GeV and 207 GeV and on R_{c} at centre-of-mass energies of 196, 200, 205 and 207 GeV are included. Table 8 summarises all the inputs that have been combined so far.

A common signal definition is defined for all the measurements, requiring:

- an effective centre-of-mass energy $\sqrt{s'} > 0.85\sqrt{s}$
- no subtraction of ISR and FSR photon interference contribution and
- extrapolation to full angular acceptance.

Systematic errors are divided into three categories: uncorrelated errors, errors correlated between the measurements of each experiment, and errors common to all experiments.

Due to the fact that R_{c} measurements are only provided by a single experiment and are strongly correlated with R_{b} measurements, it was decided to fit the b sector and c sector separately, the other flavour's measurements being fixed to their Standard Model predictions. In addition, these fitted values are used to set limits upon physics beyond the Standard Model, such

*Unlike at LEP-I, R_q^0 is defined as $\frac{\sigma_{\mathrm{q\overline{q}}}}{\sigma_{\mathrm{had}}}$.

as contact term interactions, in which only one quark flavour is assumed to be effected by the new physics during each fit, therefore this averaging method is consistent with the interpretations.

Full details concerning the combination procedure can be found in [14].

The results of the combination are presented in Table 9 and Table 10 and in Figures 7 and 8. The results for both b and c sector are in agreement with the Standard Model predictions of ZFITTER. The averaged discrepancies with respect to the Standard Model predictions is -2.08 σ for R_{b}, +0.30 σ for R_{c}, -1.56 σ for $A_{\mathrm{FB}}^{\mathrm{b\overline{b}}}$ and -0.24 σ for $A_{\mathrm{FB}}^{\mathrm{c\overline{c}}}$. A list of the error contributions from the combination at 189 GeV is shown in Table 11.

5 Interpretation

The combined measurements presented above are interpreted in a variety of models. The cross-section and asymmetry results are used to place limits on contact interactions between leptons and quarks and, using the results on heavy flavour production, on contact interaction between electrons and b and c quarks specifically. Limits on the mass of a possible additional heavy neutral boson, Z$'$, are obtained for a variety of models. The results update those provided in [1]. Using the combined differential cross-sections for $\mathrm{e^+e^-}$ final states, limits on contact interactions in the $\mathrm{e^+e^-} \to \mathrm{e^+e^-}$ channel and limits on the scale of gravity in models with large extra-dimensions are presented. Limits are also derived on the masses of leptoquarks - assuming a coupling of electromagnetic strength. In all case the Born level predictions for the physics beyond the Standard Model have been corrected to take into account QED radiation.

5.1 Contact Interactions

The averages of cross-sections and forward-backward asymmetries for muon-pair and tau-lepton pair and the cross-sections for $\mathrm{q\overline{q}}$ final states are used to search for contact interactions between fermions. The results are updated with respect to those given previously [1] due to updates of the averages. Limits are also given for interactions not considered before.

Following [17], contact interactions are parameterised by an effective Lagrangian, $\mathcal{L}_{\mathrm{eff}}$, which is added to the Standard Model Lagrangian and has the form:

$$\mathcal{L}_{\mathrm{eff}} = \frac{g^2}{(1+\delta)\Lambda^2} \sum_{i,j=L,R} \eta_{ij} \overline{e}_i \gamma_\mu e_i \overline{f}_j \gamma^\mu f_j,$$

where $g^2/4\pi$ is taken to be 1 by convention, $\delta = 1(0)$ for $f = e$ ($f \neq e$), $\eta_{ij} = \pm 1$ or 0, Λ is the scale of the contact interactions, e_i and f_j are left or right-handed spinors. By assuming different helicity coupling between the initial state and final state currents, a set of different models can be defined from this Lagrangian [18], with either constructive (+) or destructive (−) interference between the Standard Model process and the contact interactions. The models and corresponding choices of η_{ij} are given in Table 12. The models LL, RR, VV, AA, LR, RL, V0, A0 are considered here since these models lead to large deviations in $\mathrm{e^+e^-} \to \mathrm{f\overline{f}}$ at LEP II.

For leptonic final states 4 different fits are made

- individual fits to contact interaction in $\mathrm{e^+e^-} \to \mu^+\mu^-$ and $\mathrm{e^+e^-} \to \tau^+\tau^-$ using the measured cross-sections and asymmetries,
- fits to $\mathrm{e^+e^-} \to \ell^+\ell^-$, a combination of $\mathrm{e^+e^-} \to \mu^+\mu^-$ and $\mathrm{e^+e^-} \to \tau^+\tau^-$ again using the measured cross-sections and asymmetries,

$\sqrt{s}$ (GeV)	R_b				R_c				$A_{FB}^{b\bar{b}}$				$A_{FB}^{c\bar{c}}$			
	A	D	L	O	A	D	L	O	A	D	L	O	A	D	L	O
133	F	F	F	F	-	-	-	-	-	F	-	F	-	F	-	F
167	F	F	F	F	-	-	-	-	-	F	-	F	-	F	-	F
183	F	P	F	F	F	-	-	-	F	-	-	F	P	-	-	F
189	P	P	F	F	P	-	-	-	P	P	F	F	P	-	-	F
192 to 202	P	P	P	-	P*	-	-	-	P	P	-	-	-	-	-	-
205 and 207	-	P	P	-	P	-	-	-	P	P	-	-	-	-	-	-

Table 8: Data provided by the ALEPH, DELPHI, L3, OPAL collaborations for combination at different centre-of-mass energies. Data indicated with F are final, published data. Data marked with P are preliminary and for data marked with P*, not all energies are supplied. Data marked with a - were not supplied for combination.

$\sqrt{s}$ (GeV)	R_b	$A_{FB}^{b\bar{b}}$
133	0.1822 ± 0.0132 (0.1867)	0.367 ± 0.251 (0.504)
167	0.1494 ± 0.0127 (0.1727)	0.624 ± 0.254 (0.572)
183	0.1646 ± 0.0094 (0.1692)	0.515 ± 0.149 (0.588)
189	0.1565 ± 0.0061 (0.1681)	0.529 ± 0.089 (0.593)
192	0.1551 ± 0.0149 (0.1676)	0.424 ± 0.267 (0.595)
196	0.1556 ± 0.0097 (0.1670)	0.535 ± 0.151 (0.598)
200	0.1683 ± 0.0099 (0.1664)	0.596 ± 0.149 (0.600)
202	0.1646 ± 0.0144 (0.1661)	0.607 ± 0.241 (0.601)
205	0.1606 ± 0.0126 (0.1657)	0.715 ± 0.214 (0.603)
207	0.1694 ± 0.0107 (0.1654)	0.175 ± 0.156 (0.604)

Table 9: Results of R_b and $A_{FB}^{b\bar{b}}$ fit, compared to the Standard Model predictions, computed with ZFITTER [15], for the signal definition in parentheses. Quoted errors represent the statistical and systematic errors added in quadrature.

$\sqrt{s}$ (GeV)	R_c	$A_{FB}^{c\bar{c}}$
133	-	0.630 ± 0.313 (0.684)
167	-	0.980 ± 0.343 (0.677)
183	0.2628 ± 0.0397 (0.2472)	0.717 ± 0.201 (0.663)
189	0.2298 ± 0.0213 (0.2490)	0.542 ± 0.143 (0.656)
196	0.2734 ± 0.0387 (0.2508)	-
200	0.2535 ± 0.0360 (0.2518)	-
205	0.2816 ± 0.0394 (0.2530)	-
207	0.2890 ± 0.0350 (0.2533)	-

Table 10: Results of R_c and $A_{FB}^{c\bar{c}}$ fit, compared to the Standard Model predictions, computed with ZFITTER [15], for the signal definition in parentheses. Quoted errors represent the statistical and systematic errors added in quadrature.

Error list	R_b (189 GeV)	$A_{FB}^{b\bar{b}}$ (189 GeV)	R_c (189 GeV)	$A_{FB}^{c\bar{c}}$ (189 GeV)
statistics	0.00570	0.0844	0.01689	0.1186
internal syst	0.00197	0.0248	0.01090	0.0424
common syst	0.00074	0.0111	0.00715	0.0686
total syst	0.00210	0.0272	0.01303	0.0806
total error	0.00608	0.0887	0.02131	0.1434

Table 11: Error breakdown at 189 GeV.

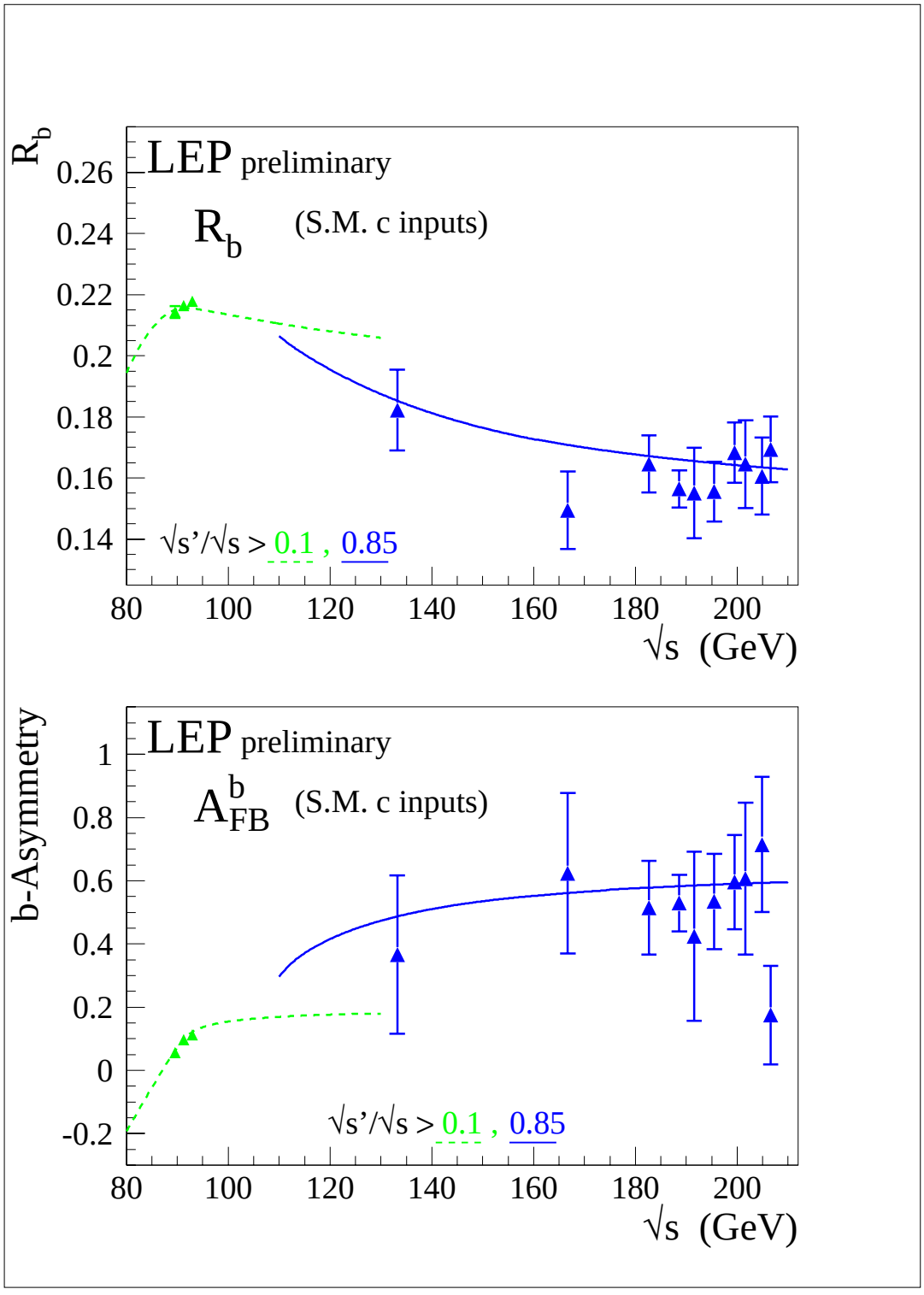

Figure 7: Preliminary combined LEP measurements of R_b and $A_{FB}^{b\bar{b}}$. Solid lines represent the Standard Model prediction for the signal definition and dotted lines the inclusive prediction. Both are computed with ZFITTER[15]. The LEP-I measurements have been taken from [16].

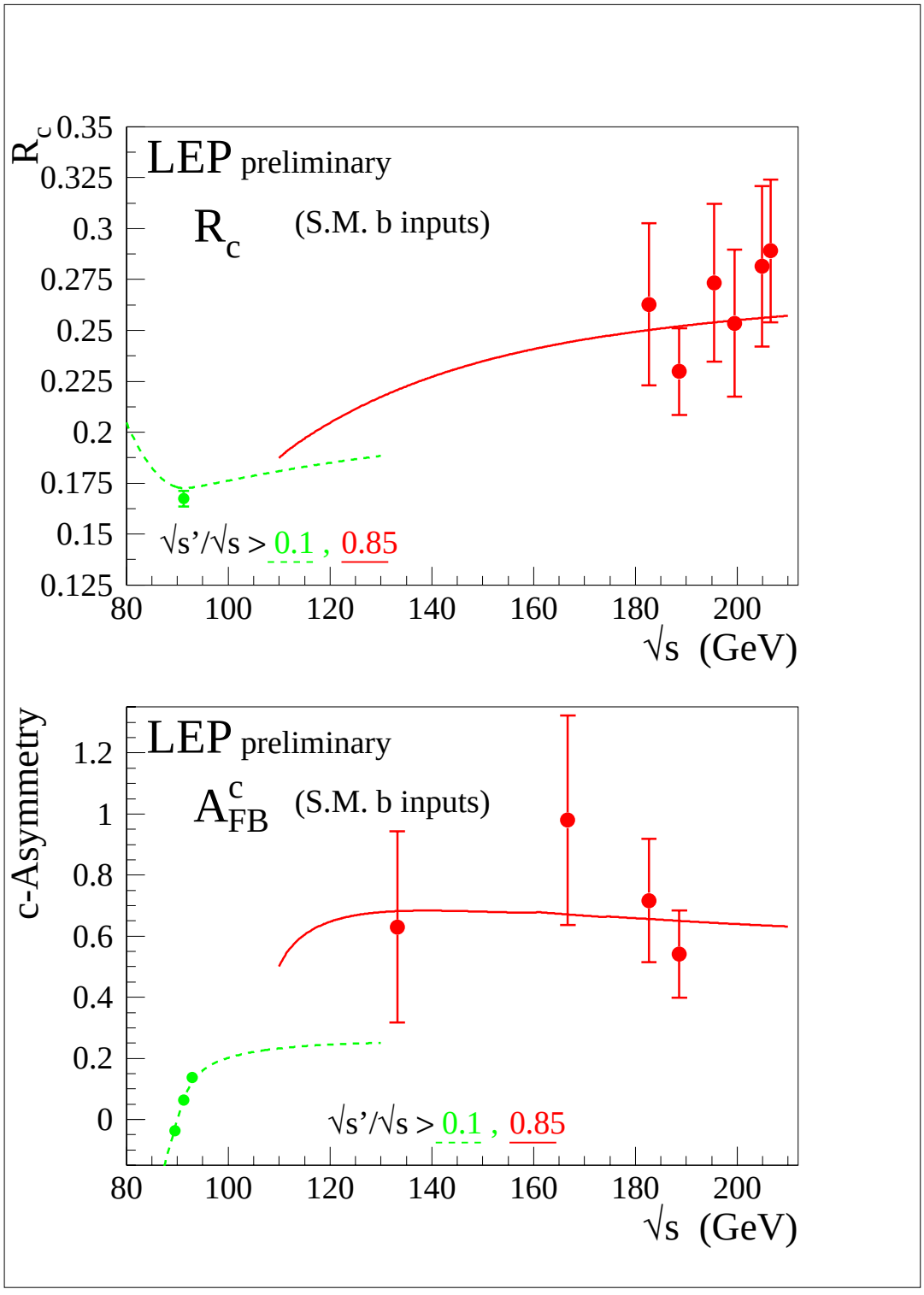

Figure 8: Preliminary combined LEP measurements of the forward–backward asymmetries R_c and $A_{FB}^{c\bar{c}}$. Solid lines represent the Standard Model prediction for the signal definition and dotted lines the inclusive prediction. Both are computed with ZFITTER [15]. The LEP-I measurements have been taken from [16].

- fits to $e^+e^- \to e^+e^-$, using the measured differential cross-sections.

For inclusive hadronic final states three different assumptions are used to fit the total hadronic cross-section

- the contact interactions affect only one quark flavour of up-type using the measured hadronic cross-sections,
- the contact interactions affect only one quark flavour of down-type using the measured hadronic cross-sections,
- the contact interactions contribute to all quark final states with the same strength.

Limits on contact interactions between electrons and b and c quarks are obtained using all the heavy flavour LEP-II combined results from 133 GeV to 207 GeV given in Tables 9 and 10. For the purpose of fitting contact interaction models to the data, R_b and R_c are converted to cross-sections $\sigma_{b\overline{b}}$ and $\sigma_{c\overline{c}}$ using the averaged $q\overline{q}$ cross-section of section 2 corresponding to the second signal definition. In the calculation of errors, the correlations between R_b, R_c and $\sigma_{q\overline{q}}$ are assumed to be negligible. These results are of particular interest since they are inaccessible to $p\bar{p}$ or ep colliders.

For the purpose of fitting contact interaction models to the data, a new parameter $\epsilon = 1/\Lambda^2$ is defined; $\epsilon = 0$ in the limit that there are no contact interactions. This parameter is allowed to take both positive and negative values in the fits. Theoretical uncertainties on the Standard Model predictions are taken from [9].

The values of ϵ extracted for each model are all compatible with the Standard Model expectation $\epsilon = 0$, at the two standard deviation level. These errors on ϵ are typically a factor of two smaller than those obtained from a single LEP experiment with the same data set. The fitted values of ϵ are converted into 95% confidence level lower limits on Λ. The limits are obtained by integrating the likelihood function over the physically allowed values[†], $\epsilon \geq 0$ for each Λ^+ limit and $\epsilon \leq 0$ for Λ^- limits.

The fitted values of ϵ and their 68% confidence level uncertainties together with the 95% confidence level lower limit on Λ are shown in Table 13 for the fits to $e^+e^- \to \ell^+\ell^-$ ($\ell \neq e$), $e^+e^- \to e^+e^-$, inclusive $e^+e^- \to q\overline{q}$, $e^+e^- \to b\overline{b}$ and $e^+e^- \to c\overline{c}$. Table 14 shows only the limits obtained on the scale Λ for other fits. The limits are shown graphically in Figure 9.

For the VV model with positive interference and assuming electromagnetic coupling strength instead of $g^2/4\pi = 1$, the scale Λ obtained in the $e^+e^- \to e^+e^-$ channel is converted to an upper limit on the electron size:

$$r_e < 1.4 \times 10^{-19} \mathrm{m}$$

Models with stronger couplings will make this upper limit even tighter.

5.2 Models with Z′ Bosons

The combined hadronic and leptonic cross-sections and the leptonic forward-backward asymmetries are used to fit the data to models including an additional, heavy, neutral boson, Z′. The results are updated with respect to those given in [1] due to the updated cross-section and leptonic forward-backward asymmetry results.

[†]To be able to obtain confidence limits from the likelihood function it is necessary to convert the likelihood to a probability density function; this is done by multiplying by a prior probability function. Simply integrating the likelihood is equivalent to multiplying by a uniform prior probability function.

Model	η_{LL}	η_{RR}	η_{LR}	η_{RL}
$LL^{\pm}$	± 1	0	0	0
$RR^{\pm}$	0	± 1	0	0
$VV^{\pm}$	± 1	± 1	± 1	± 1
$AA^{\pm}$	± 1	± 1	∓ 1	∓ 1
$LR^{\pm}$	0	0	± 1	0
$RL^{\pm}$	0	0	0	± 1
$V0^{\pm}$	± 1	± 1	0	0
$A0^{\pm}$	0	0	± 1	± 1

Table 12: Choices of η_{ij} for different contact interaction models

.

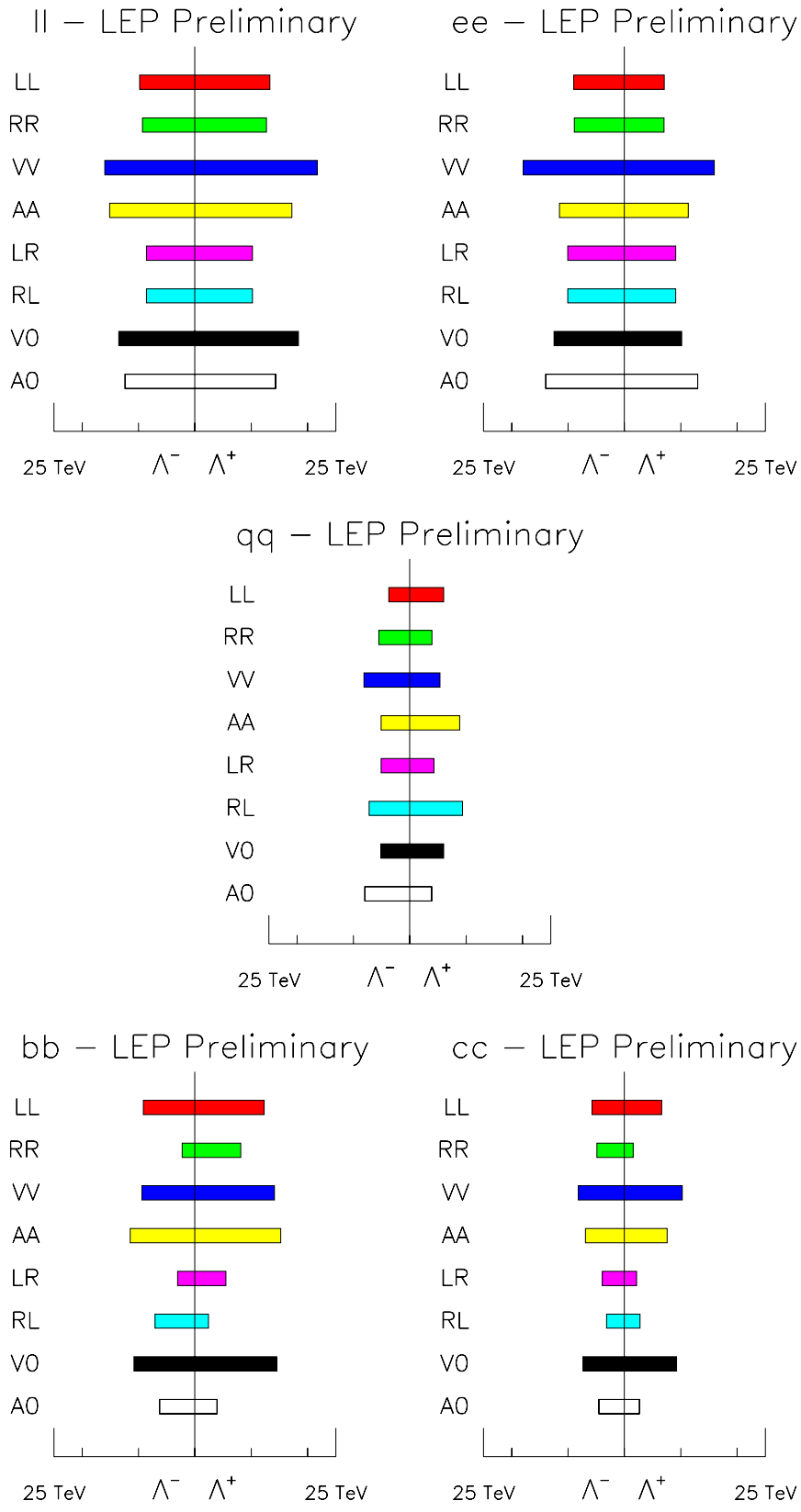

Figure 9: The limits on Λ for $e^+e^- \to \ell^+\ell^-$ assuming universality in the contact interactions between $e^+e^- \to \ell^+\ell^-$ ($\ell \neq e$), for $e^+e^- \to e^+e^-$, for $e^+e^- \to q\overline{q}$ assuming equal strength contact interactions for quarks and for $e^+e^- \to b\overline{b}$ and $e^+e^- \to c\overline{c}$.

$e^+e^- \to \ell^+\ell^-$			
Model	ϵ (TeV^{-2})	Λ^- (TeV)	Λ^+ (TeV)
LL	$-0.0044^{+0.0035}_{-0.0035}$	9.8	13.3
RR	$-0.0049^{+0.0039}_{-0.0039}$	9.3	12.7
VV	$-0.0016^{+0.0013}_{-0.0014}$	16.0	21.7
AA	$-0.0013^{+0.0017}_{-0.0017}$	15.1	17.2
LR	$-0.0036^{+0.0052}_{-0.0054}$	8.6	10.2
RL	$-0.0036^{+0.0052}_{-0.0054}$	8.6	10.2
V0	$-0.0023^{+0.0018}_{-0.0018}$	13.5	18.4
A0	$-0.0018^{+0.0026}_{-0.0026}$	12.4	14.3

$e^+e^- \to e^+e^-$			
Model	ϵ (TeV^{-2})	Λ^- (TeV)	Λ^+ (TeV)
LL	$0.0049^{+0.0084}_{-0.0084}$	9.0	7.1
RR	$0.0056^{+0.0082}_{-0.0092}$	8.9	7.0
VV	$0.0004^{+0.0022}_{-0.0016}$	18.0	15.9
AA	$0.0009^{+0.0041}_{-0.0039}$	11.5	11.3
LR	$0.0008^{+0.0064}_{-0.0052}$	10.0	9.1
RL	$0.0008^{+0.0064}_{-0.0052}$	10.0	9.1
V0	$0.0028^{+0.0038}_{-0.0045}$	12.5	10.2
A0	$-0.0008^{+0.0028}_{-0.0030}$	14.0	13.0

$e^+e^- \to q\overline{q}$			
Model	ϵ (TeV^{-2})	Λ^- (TeV)	Λ^+ (TeV)
LL	$0.0152^{+0.0064}_{-0.0076}$	3.7	6.0
RR	$-0.0208^{+0.0103}_{-0.0082}$	5.5	3.9
VV	$-0.0096^{+0.0051}_{-0.0037}$	8.1	5.3
AA	$0.0068^{+0.0033}_{-0.0034}$	5.1	8.8
LR	$-0.0308^{+0.0172}_{-0.0055}$	5.1	4.3
RL	$-0.0108^{+0.0057}_{-0.0054}$	7.2	9.3
V0	$0.0174^{+0.0057}_{-0.0074}$	5.1	6.0
A0	$-0.0092^{+0.0049}_{-0.0041}$	8.0	3.9

$e^+e^- \to b\overline{b}$			
Model	ϵ (TeV^{-2})	Λ^- (TeV)	Λ^+ (TeV)
LL	$-0.0038^{+0.0044}_{-0.0047}$	9.1	12.3
RR	$-0.1729^{+0.1584}_{-0.0162}$	2.2	8.1
VV	$-0.0040^{+0.0039}_{-0.0041}$	9.4	14.1
AA	$-0.0022^{+0.0029}_{-0.0031}$	11.5	15.3
LR	$-0.0620^{+0.0692}_{-0.0313}$	3.1	5.5
RL	$0.0180^{+0.1442}_{-0.0249}$	7.0	2.4
V0	$-0.0028^{+0.0032}_{-0.0033}$	10.8	14.5
A0	$0.0375^{+0.0193}_{-0.0379}$	6.3	3.9

$e^+e^- \to c\overline{c}$			
Model	ϵ (TeV^{-2})	Λ^- (TeV)	Λ^+ (TeV)
LL	$-0.0091^{+0.0126}_{-0.0126}$	5.7	6.6
RR	$0.3544^{+0.0476}_{-0.3746}$	4.9	1.5
VV	$-0.0047^{+0.0057}_{-0.0060}$	8.2	10.3
AA	$-0.0059^{+0.0095}_{-0.0090}$	6.9	7.6
LR	$0.1386^{+0.0555}_{-0.1649}$	3.9	2.1
RL	$0.0106^{+0.0848}_{-0.0757}$	3.1	2.8
V0	$-0.0058^{+0.0075}_{-0.0071}$	7.4	9.2
A0	$0.0662^{+0.0564}_{-0.0905}$	4.5	2.7

Table 13: The fitted values of ϵ and the derived 95% confidence level lower limits on the parameter Λ of contact interaction derived from fits to lepton-pair cross-sections and asymmetries and from fits to hadronic cross-sections. The limits Λ_+ and Λ_- given in TeV correspond to the upper and lower signs of the parameters η_{ij} in Table 12. For $\ell^+\ell^-$ ($\ell \neq e$) the couplings to $\mu^+\mu^-$ and $\tau^+\tau^-$ are a assumed to be universal and for inclusive $q\overline{q}$ final states all quarks are assumed to experience contact interactions with the same strength.

leptons				
	$\mu^+\mu^-$		$\tau^+\tau^-$	
Model	Λ_-	Λ_+	Λ_-	Λ_+
LL	8.5	12.5	9.1	8.6
RR	8.1	11.9	8.7	8.2
VV	14.3	19.7	14.2	14.5
AA	12.7	16.4	14.0	11.3
LR	7.9	8.9	2.2	7.9
RL	7.9	8.9	2.2	7.9
V0	11.7	17.2	12.7	11.8
A0	11.5	12.4	9.8	10.8

hadrons				
	up-type		down-type	
Model	Λ_-	Λ_+	Λ_-	Λ_+
LL	6.7	10.2	10.6	6.0
RR	5.7	8.3	2.2	4.3
VV	9.6	14.3	11.4	7.0
AA	8.0	11.5	13.3	7.7
LR	4.2	2.3	2.7	3.5
RL	3.5	2.8	4.2	2.4
V0	8.7	13.4	12.5	7.1
A0	4.9	2.8	4.2	3.3

Table 14: The 95% confidence level lower limits on the parameter Λ of contact interaction derived from fits to lepton-pair cross-sections and asymmetries and from fits to hadronic cross-sections. The limits Λ_+ and Λ_- given in TeV correspond to the upper and lower signs of the parameters η_{ij} in Table 12. For hadrons the limits for up-type and down-type quarks are derived assuming a single up or down type quark undergoes contact interactions.

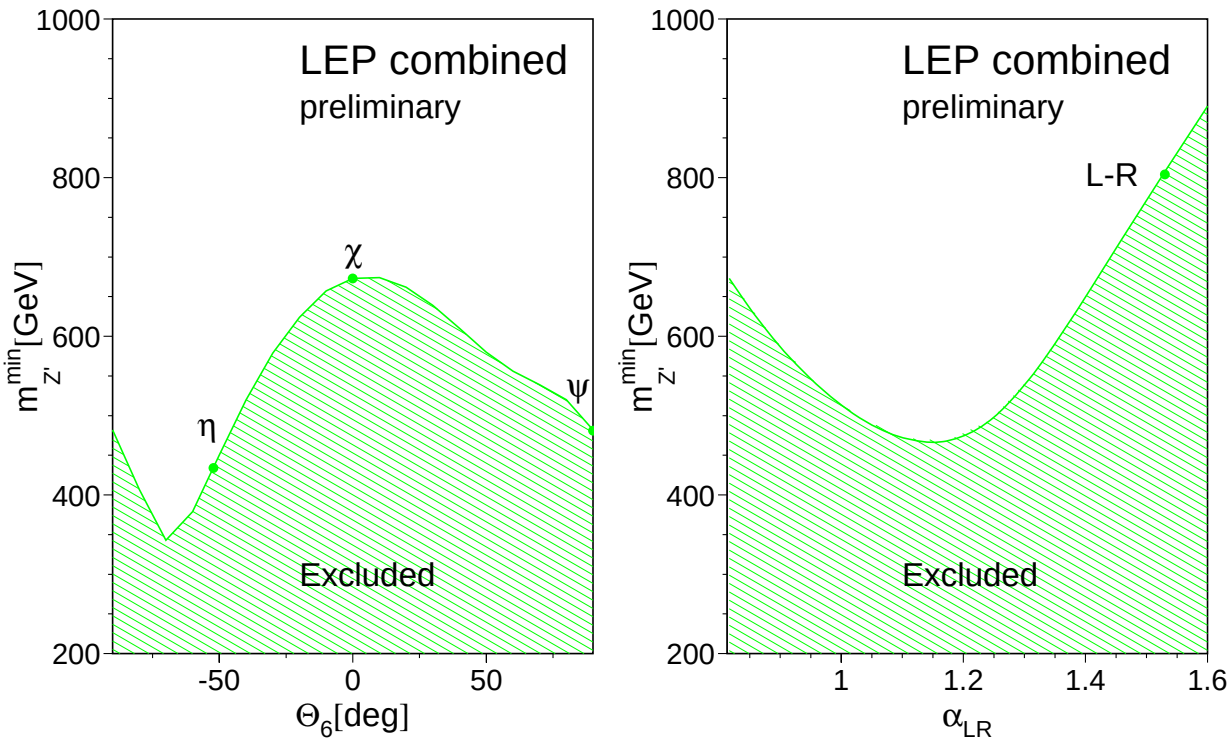

Figure 10: The 95% confidence level limits on $M_{Z'}$ as a function of the model parameter θ_6 for E_6 models and α_{LR} for left-right models. The Z-Z′ mixing is fixed, $\Theta_{ZZ'} = 0$.

Z′ model	χ	ψ	η	L-R	SSM
$M^{limit}_{Z'}$ (GeV/c^2)	673	481	434	804	1787

Table 15: The 95% confidence level lower limits on the Z′ mass for χ, ψ, η, L-R and SSM models.

Fits are made to the mass of a Z′, $M_{Z'}$, for models resulting from an E_6 GUT and L-R symmetric models [19] and for the Sequential Standard Model [20], which proposes the existence of a Z′ with exactly the same coupling to fermions as the standard Z. LEP-II data alone does not significantly constrain the mixing angle between the Z and Z′ fields, $\Theta_{ZZ'}$. However results from a single experiment, in which LEP-I data is used in the fit, show that the mixing is consistent with zero (see for example [21]). So for these fits $\Theta_{ZZ'}$ was fixed to zero.

No significant evidence is found for the existence of a Z′ boson in any of the models. The procedure to find limits on the Z′ mass corresponds to that in case of contact interactions: for large masses the exchange of a Z′ can be approached by contact terms, $\Lambda \propto M_{Z'}$. The lower limits on the Z′ mass are shown in Figure 10 varying the parameters θ_6 for the E_6 models and α_{LR} for the left-right models. The results for the specific models χ, ψ ,η ($\theta_6 = 0,\ \pi/2,\ -\arctan\sqrt{5/3}$), L-R ($\alpha_{LR}$=1.53) and SSM are shown in Table 15.

5.3 Leptoquarks and R-parity violating squarks

Leptoquarks (LQ) would mediate quark-lepton transitions. Following the notations in Reference [22, 23], scalar leptoquarks, S_I, and vector leptoquarks,V_I are indicated based on spin and isospin I. Isomultiplets with different hypercharges are denoted by an additional tilde. They carry fermion numbers, $F = L + 3B$. It is assumed that leptoquark couplings to quark-lepton

pairs preserve baryon- and lepton-number. The couplings g_L, g_R, are labelled according to the chirality of the lepton.

$\tilde{\mathrm{S}}_{1/2}$(L) and S_0(L) leptoquarks are equivalent to up-type anti-squarks and down-type squarks, respectively. Limits in terms of the leptoquark coupling are then exactly equivalent to limits on λ_{1jk} in the Lagrangian $\lambda_{1jk}L_1Q_j\bar{D}_k$.

At LEP, the exchange of a leptoquark can modify the hadronic cross-sections and asymmetries, as described by the Born level of equations given in [23]. Using the LEP combined measurements of hadronic cross-sections, and the measurements of heavy quark production, R_{b}, R_{c}, $A_{\mathrm{FB}}^{\mathrm{b\overline{b}}}$ and $A_{\mathrm{FB}}^{\mathrm{c\overline{c}}}$, upper limits can be set on the leptoquark's coupling g as a function of its mass M_{LQ} for leptoquarks coupling electrons to first, second and third generation quarks. For convenience, one type of leptoquark is assumed to be much lighter than the others. Furthermore, experimental constraints on the product g_Lg_R allow the separate study of $g_L \neq 0$ or $g_R \neq 0$.

In the processes $\mathrm{e^+e^-} \to \mathrm{u\overline{u}}$ and $\mathrm{e^+e^-} \to \mathrm{d\overline{d}}$ first generation leptoquarks could be exchanged in u- or t-channel (F=2 or F=0) which would lead to a change of the hadronic cross-section. In the processes $\mathrm{e^+e^-} \to \mathrm{c\overline{c}}$ and $\mathrm{e^+e^-} \to \mathrm{b\overline{b}}$ the exchange of leptoquarks with cross-generational couplings can alter the $\mathrm{q\overline{q}}$ angular distribution, especially at low polar angle. The reported measurements on heavy quark production have been extrapolated to 4π acceptance, using SM predictions, from the measurements performed in restricted angular ranges, corresponding to the acceptance of the vertex-detector in each experiment. Therefore, when fitting limits on leptoquarks' coupling to the 2nd or 3rd generation of quarks, the LEP combined results for b and c sector are extrapolated back to an angular range of $|\cos\theta| < 0.85$ using ZFITTER predictions.

The following measurements are used to constrain different types of leptoquarks

- For leptoquarks coupling electrons to 1^{st} generation quarks, all LEP combined hadronic cross-sections at centre-of-mass energies from 130 GeV to 207 GeV are used

- For leptoquarks coupling electrons to 2^{nd} generation quarks, $\sigma_{\mathrm{c\overline{c}}}$ is calculated from R_{c} and the hadronic cross-section at the energy points where R_{c} is measured. The measurements of $\sigma_{\mathrm{c\overline{c}}}$ and $A_{\mathrm{FB}}^{\mathrm{c\overline{c}}}$ are then extrapolated back to $|\cos\theta| < 0.85$. Since measurements in the c-sector are scarce and originate from, at most, 2 experiments, hadronic cross-sections, extrapolated down to $|\cos\theta| < 0.85$ are also used in the fit, with an average 10% correlated errors.

- For leptoquarks coupling electrons to 3^{rd} generation quarks, only $\sigma_{b\bar{b}}$ and $A_{\mathrm{FB}}^{\mathrm{b\overline{b}}}$, extrapolated back to a $|\cos\theta| < 0.85$ are used.

The 95% confidence level lower limits on masses M_{LQ} are derived assuming a coupling of electromagnetic strength, $g = \sqrt{4\pi\alpha_{em}}$, where α_{em} is the fine structure constant. The results are summarised in Table 16. These results complement the leptoquark searches at HERA [24,25] and the Tevatron [26]. Figures 11 and 12 give the 95% confidence level limits on the coupling as a function of the leptoquark mass for leptoquarks coupling electrons to the second and third generations of quarks.

5.4 Low Scale Gravity in Large Extra Dimensions

The averaged differential cross-sections for $\mathrm{e^+e^-} \to \mathrm{e^+e^-}$ are used to search for the effects of graviton exchange in large extra dimensions.

Limit on scalar LQ mass (GeV/c^2)							
	S_0(L)	S_0(R)	$\tilde{S}_0$(R)	$S_{\frac{1}{2}}$(L)	$S_{\frac{1}{2}}$(R)	$\tilde{S}_{\frac{1}{2}}$(L)	S_1(L)
LQ_{1st}	655	520	202	178	232	-	361
LQ_{2nd}	762	625	209	215	185	-	408
LQ_{3rd}	NA	NA	454	NA	-	226	1036

Limit on vector LQ mass (GeV/c^2)							
	V_0(L)	V_0(R)	$\tilde{V}_0$(R)	$V_{\frac{1}{2}}$(L)	$V_{\frac{1}{2}}$(R)	$\tilde{V}_{\frac{1}{2}}$(L)	V_1(L)
LQ_{1st}	917	165	489	303	227	176	659
LQ_{2nd}	968	147	478	165	466	101	687
LQ_{3rd}	765	167	NA	208	499	NA	765

Table 16: 95% confidence level lower limits on the LQ mass for leptoquarks coupling between electrons and the first, second and third generation of quarks. A dash indicates that no limit can be set and N.A denotes leptoquarks coupling only to top quarks and hence not visible at LEP.

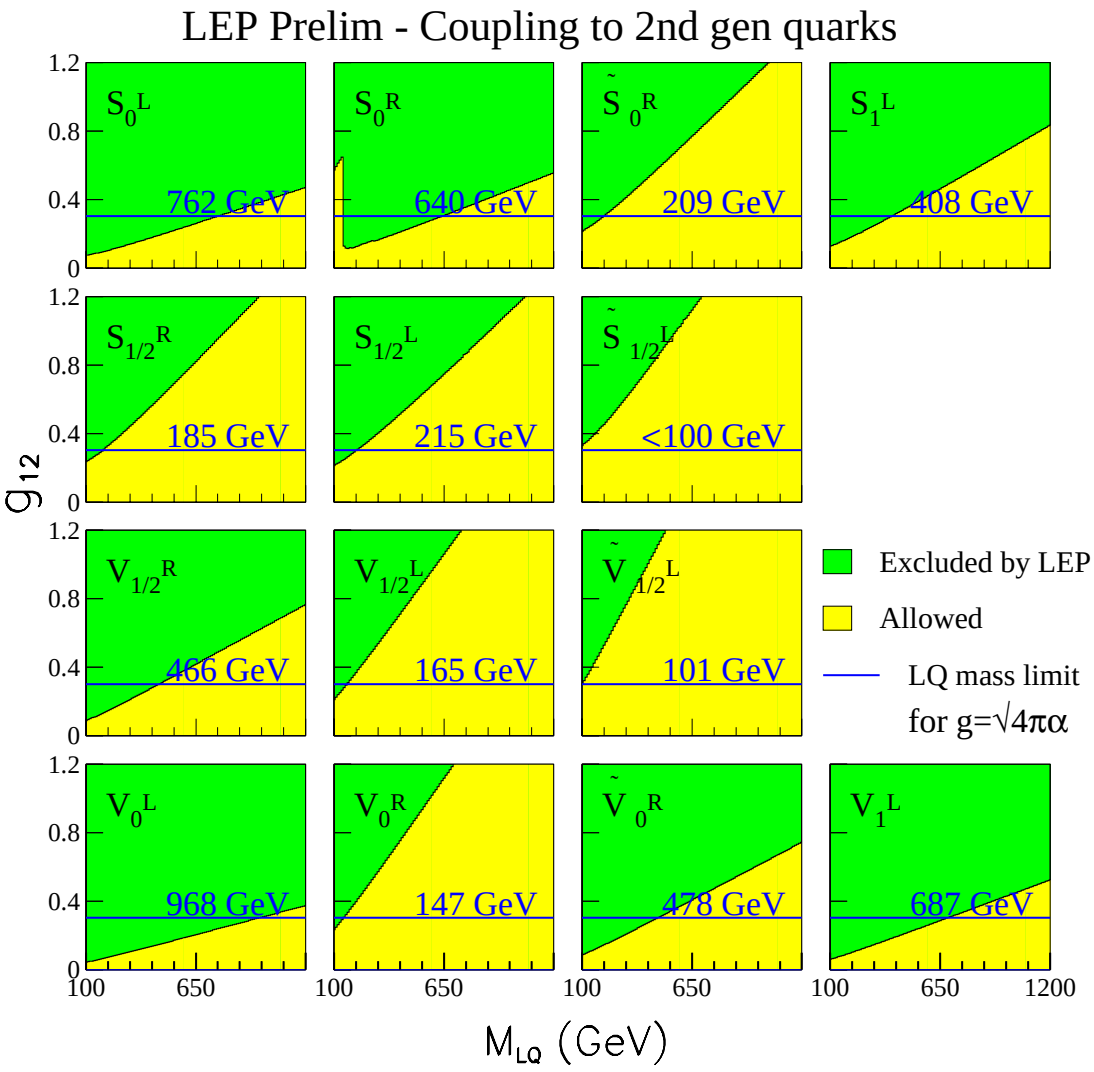

Figure 11: 95% confidence level limit on the coupling of leptoquarks to 2nd generation of quarks.

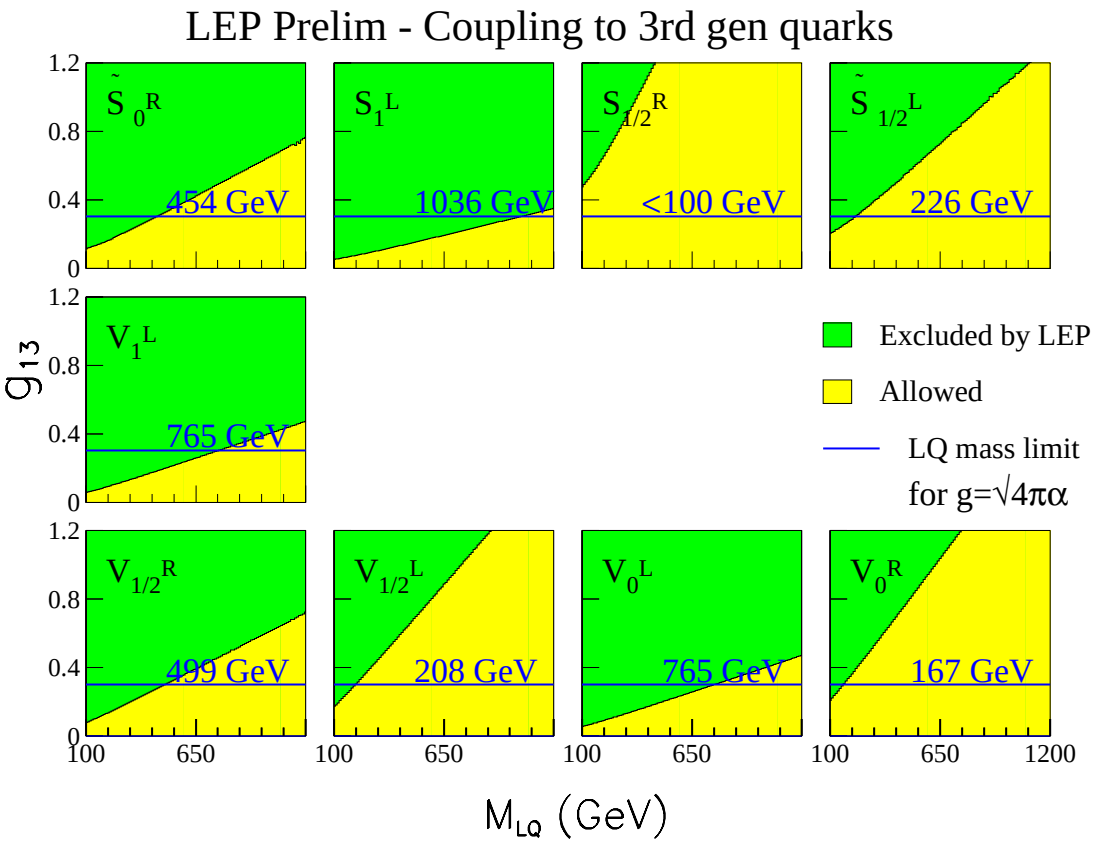

Figure 12: 95% confidence level limit on the coupling of leptoquarks to 3rd generation of quarks.

A new approach to the solution of the hierarchy problem has been proposed in [27–29], which brings close the electroweak scale $m_{EW} \sim 1$ TeV and the Planck scale $M_{Pl} = \frac{1}{\sqrt{G_N}} \sim 10^{15}$ TeV. In this framework the effective 4 dimensional M_{Pl} is connected to a new $M_{Pl(4+n)}$ scale in a (4+n) dimensional theory:

$$M_{Pl}^2 \sim M_{Pl(4+n)}^{2+n} R^n,$$

where there are n extra compact spatial dimensions of radius $\sim$ R.

In the production of fermion- or boson-pairs in e^+e^- collisions this class of models can be manifested through virtual effects due to the exchange of gravitons (Kaluza-Klein excitations). As discussed in [30–34], the exchange of spin-2 gravitons modifies in a unique way the differential cross sections for fermion pairs, providing clear signatures. These models introduce an effective scale (ultraviolet cut-off). Adopting the notation from [30] the gravitational mass scale is called M_H. The cut-off scale is supposed to be of the order of the fundamental gravity scale in 4+n dimensions.

The parameter ε is defined as

$$\varepsilon = \frac{\lambda}{M_H^4},$$

where the coefficient λ is of $\mathcal{O}(1)$ and can not be calculated explicitly without knowledge of the full quantum gravity theory. In the following analysis we will assume that $\lambda = \pm 1$ in order to study both the cases of positive and negative interference. To compute the deviations from the Standard Model due to virtual graviton exchange the calculations [31, 32] were used.

Theoretical uncertainties on the Standard Model predictions are taken from [9]. The full correlation matrix of the differential cross-sections, obtained in our averaging procedure, is used in the fits. This is an improvement compared to previous combined analyses of published or preliminary LEP data on Bhabha scattering, performed before this detailed information was available (see e.g. [35–37]).

The extracted value of ε is compatible with the Standard Model expectation $\varepsilon = 0$. The errors on ε are ~ 1.5 smaller than those obtained from a single LEP experiment with the same data set. The fitted value of ε is converted into 95% confidence level lower limits on M_H by integrating the likelihood function over the physically allowed values, $\varepsilon \geq 0$ for λ^+ and $\varepsilon \leq 0$ for λ^- giving:

$$M_H > 1.20 \text{ TeV for } \lambda = +1;$$
$$M_H > 1.09 \text{ TeV for } \lambda = -1.$$

An example of our analysis for the highest energy point is shown in Figure 13.

The interference of virtual graviton exchange amplitudes with both t-channel and s-channel Bhabha scattering amplitudes makes this the most sensitive search channel at LEP. The results obtained here would not be strictly valid if the luminosity measurements of the LEP experiments, based on the very same process, are also significantly affected by graviton exchange. As shown in [35], the effect on the cross section in the luminosity angular range is so small that it can safely be neglected in this analysis.

6 Summary

A preliminary combination of the LEP-II $e^+e^- \to f\bar{f}$ cross-sections (for hadron, muon and tau-lepton final states) and forward-backward asymmetries (for muon and tau final states) from LEP running at energies from 130 GeV to 207 GeV has been made. The results from the four LEP

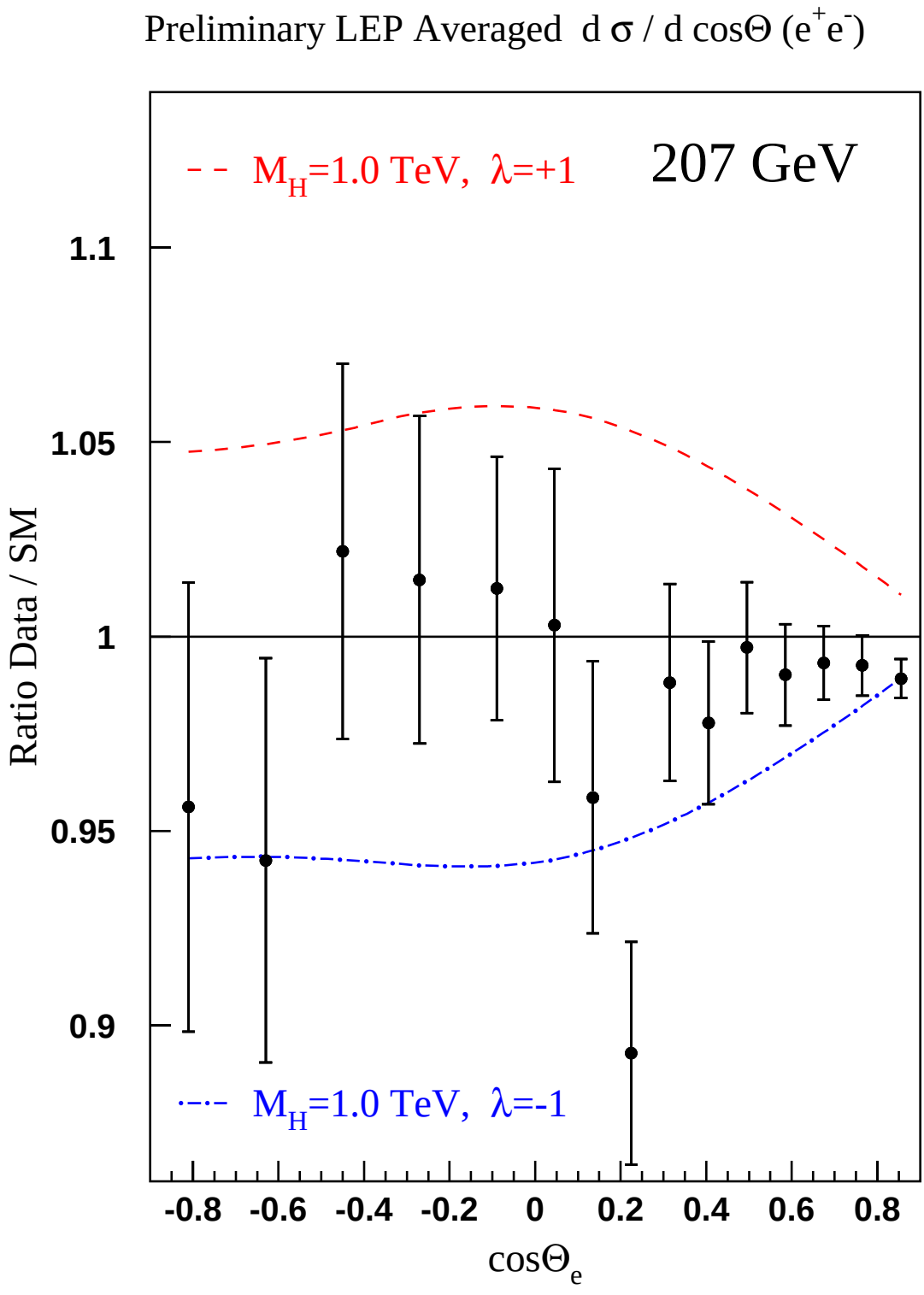

Figure 13: Ratio of the LEP averaged differential cross-section for $e^+e^- \to e^+e^-$ at energy of 207 GeV compared to the SM prediction. The effects expected from virtual graviton exchange are also shown.

experiments are in good agreement with each other. The averages for all energies are shown given in Table 2. Overall the data agree with the Standard Model predictions of ZFITTER, although the combined hadronic cross-sections are on average 1.7 standard deviations above the predictions. Further information is available at [6].

Preliminary differential cross-sections, $\frac{\mathrm{d}\sigma}{\mathrm{d}\cos\theta}$, for $\mathrm{e^+e^-} \to \mathrm{e^+e^-}$, $\mathrm{e^+e^-} \to \mu^+\mu^-$ and $\mathrm{e^+e^-} \to \tau^+\tau^-$ were combined. Results are shown in Figures 4, 5 and 6.

A preliminary average of results on heavy flavour production at LEP-II has also been made for measurements of R_b, R_c, $A_{\mathrm{FB}}^{\mathrm{b\overline{b}}}$ and $A_{\mathrm{FB}}^{\mathrm{c\overline{c}}}$, using results from LEP centre-of-mass energies from 130 to 207 GeV. Results are given in Tables 9 and 10 and shown graphically in Figures 7 and 8. The results are in good agreement with the predictions of the SM.

The preliminary averaged cross-section and forward-backward asymmetry results together with the combined results on heavy flavour production have been interpreted in a variety of models. Limits on the scale of contact interactions between leptons and quarks and in $\mathrm{e^+e^-} \to \mathrm{e^+e^-}$ and also between electrons and specifically $\mathrm{b\overline{b}}$ and $\mathrm{c\overline{c}}$ final states have been determined. A full set of limits are given in Tables 13 and 14. The LEP-II averaged cross-sections have been used to obtain lower limits on the mass of a possible Z' boson in different models. Limits range from 340 to 1787 GeV/c^2 depending on the model. Limits on the masses of leptoquarks have been derived from the hadronic cross-sections. The limits range from 101 to 1036 GeV/c^2 depending on the type of leptoquark. Limits on the scale of gravity in models with large extra dimensions have been obtained from combined differential cross-sections for $\mathrm{e^+e^-} \to \mathrm{e^+e^-}$; for positive interference between the new physics and the Standard model the limit is 1.20 TeV and for negative interference 1.09 TeV.

Acknowledgements

The analysis and interpretation of the high energy $\mathrm{f\overline{f}}$ data requires the theoretical input from Monte Carlo programs to compute efficiencies, from programs to compute the luminosity and programs which make Standard Model predictions. We would like to acknowledge the work of all the authors of these programs. In particular we are grateful to D. Bardin, S. Jadach, G. Passarino and B. Ward for their direct contributions to our work.

References

[1] LEPEWWG $f\bar{f}$ Subgroup, C. Geweniger *et. al.*, LEP2FF/01-02,ALEPH 2001-076 PHYSIC 2001-026, DELPHI 2001-168 PHYS 904, L3 note 2712, OPAL TN704.

[2] LEPEWWG $f\bar{f}$ Subgroup, D. Bourilkov *et. al.*, LEP2FF/01-01,ALEPH 2001-039 PHYSIC 2000-013, DELPHI 2001-108 PHYS 896, L3 note 2663, OPAL TN690.

[3] LEPEWWG $f\bar{f}$ Subgroup, C. Geweniger *et. al.*, LEP2FF/00-03,ALEPH 2000-088 PHYSIC 2000-034, DELPHI 2000-168 PHYS 881, L3 note 2624, OPAL TN673.

[4] LEPEWWG $f\bar{f}$ Subgroup, D. Bourilkov *et. al.*, LEP2FF/00-01,ALEPH 2000-026 PHYSIC 2000-005, DELPHI 2000-046 PHYS 855, L3 note 2527, OPAL TN647.

[5] LEPEWWG $f\bar{f}$ Subgroup, D. Bourilkov *et. al.*, LEP2FF/99-01,ALEPH 99-082 PHYSIC 99-030, DELPHI 99-143 PHYS 829, L3 note 2443, OPAL TN616.

[6] LEPEWWG $f\bar{f}$ subgroup: http://www.cern.ch/LEPEWWG/lep2/ .

[7] ALEPH Collaboration "Study of Fermion Pair Production in e^+e^- Collisions at 130-183 GeV", Eur. Phys. J. **C12** (2000) 183;
ALEPH Collaboration, "Fermion Pair Production in e^+e^- Collisions at 189 GeV and Kimits on Physics Beyond the Standard Model", ALEPH 99-018 CONF 99-013;
ALEPH Collaboration, "Fermion Pair Production in e^+e^- Collisions from 192 to 202 GeV", ALEPH 2000-025 CONF 2000-021;
ALEPH Collaboration, "Fermion Pair Production in e^+e^- Collisions at high energy and Limits on Physics beyond the Standard Model ", ALEPH 2001-019 CONF 2001-016;
DELPHI Collaboration,"Measurement and Interpretation of Fermion-Pair Production at LEP energies from 130 to 172 GeV", Eur. Phys. J. **C11** (1999), 383;
DELPHI Collaboration, "Measurement and Interpretation of Fermion-Pair Production at LEP Energies from 183 to 189 GeV", Phys.Lett. **B485** (2000), 45;
DELPHI Collaboration, "Results on Fermion-Pair Production at LEP running from 192 to 202 GeV", DELPHI 2000-128 OSAKA CONF 427;
DELPHI Collaboration, "Results on Fermion-Pair Production at LEP running in 2000", DELPHI 2001-094 CONF 522;
L3 Collaboration, "Measurement of Hadron and Lepton-Pair Production at 161 GeV $< \sqrt{s} <$ 172 GeV at LEP", Phys. Lett. **B407** (1997) 361;
L3 Collaboration, "Measurement of Hadron and Lepton-Pair Production at 130 GeV $< \sqrt{s} <$ 189 GeV at LEP", Phys. Lett. **B479** (2000), 101.
L3 Collaboration, "Preliminary L3 Results on Fermion-Pair Production in 1999", L3 note 2563;
L3 Collaboration,"Preliminary L3 Results on Fermion-Pair Production in 2000", L3 note 2648;
OPAL Collaboration, "Tests of the Standard Model and Constraints on New Physics from Measurements of Fermion Pair Production at 130 - 172 GeV at LEP", Euro. Phys. J. **C2** (1998) 441;
OPAL Collaboration, "Tests of the Standard Model and Constraints on New Physics from Measurements of Fermion Pair Production at 183 GeV at LEP", Euro. Phys. J. **C6** (1999) 1;
OPAL Collaboration, "Tests of the Standard Model and Constraints on New Physics from Measurements of Fermion Pair Production at 189 GeV at LEP", Euro. Phys. J. **C13** (2000) 553;

OPAL Collaboration, "Tests of the Standard Model and Constraints on New Physics from Measurements of Fermion Pair Production at 192-202 GeV at LEP", OPAL PN424 (2000); OPAL Collaboration, "Measurement of Standard Model Processes in e+e- Collisions at sqrts 203-209 GeV", OPAL PN469 (2001).

[8] D. Bardin *et al.*, CERN-TH 6443/92; http://www.ifh.de/∼riemann/Zfitter/zf.html . Predictions are from ZFITTER versions 6.04 or later.
Definition 1 corresponds to the ZFITTER flags FINR=0 and INTF=0; definition 2 corresponds to FINR=0 and INTF=1 for hadrons, FINR=1 and INTF=1 for leptons.

[9] M. Kobel *et al.*, "Two-Fermion Production in Electron Positron Collisions" in S. Jadach *et al.* [eds] , "Reports of the Working Groups on Precision Calculations for LEP2 Physics: proceedings" CERN 2000-009, hep-ph/0007180.

[10] L. Lyons *et al.*, Nucl. Inst. Meth. **A270** (1988) 110.

[11] S. Jadach, W. Placzek and B.Ward, Phys. Lett. **B390** (1997) 298.

[12] ALEPH Collaboration, Euro. Phys J. **C12** (2000) 183;
DELPHI Collaboration, P.Abreu *et al.*, Euro. Phys J. **C11**(1999);
L3 Collaboration, M.Acciarri *et al.*, Phys. Lett. **B485** (2000) 71;
OPAL Collaboration, G.Abbiendi *et al.*, Euro. Phys. J. **C16** (2000) 41.

[13] ALEPH Collaboration, ALEPH 99-018 CONF 99-013;
ALEPH Collaboration, ALEPH 2000-046 CONF 2000-029;
ALEPH Collaboration, ICHEP2002, ABS388;
DELPHI Collaboration, DELPHI 2001-095 CONF 523;
L3 Collaboration, L3 Internal note 2640, 1 March 2001.

[14] LEPEWWG Heavy Flavour at LEP2 Subgroup, "Combination of Heavy Flavour Measurements at LEP2", LEP2FF/00-02.

[15] ZFITTER V6.23 is used.
D. Bardin *et al.*, Preprint hep-ph/9908433.
Relevant ZFITTER settings used are FINR=0 and INTF=1.

[16] DELPHI Collaboration, P.Abreu *et al.*, Euro Phys J. **C10**(1999) 415.
The LEP collaborations *et al.*, CERN-EP/2000-016.

[17] E. Eichten, K. Lane, and M. Peskin, Phys. Rev. Lett. **50** (1983) 811.

[18] H. Kroha, Phys. Rev. **D46** (1992) 58.

[19] P. Langacker, R.W. Robinett and J.L. Rosner, Phys. Rev. **D30** (1984) 1470;
D. London and J.L. Rosner, Phys. Rev. **D34** (1986) 1530;
J.C. Pati and A. Salam, Phys. Rev. **D10** (1974) 275;
R.N. Mohapatra and J.C. Pati, Phys. Rev. **D11** (1975) 566.

[20] G. Altarelli *et al.*, Z. Phys. **C45** (1989) 109;
erratum Z. Phys. **C47** (1990) 676.

[21] DELPHI Collaboration, P. Abreu *et al.*, Zeit. Phys. **C65** (1995) 603.

[22] W. Buchmüller, R. Rückl, D. Wyler, Phys. Lett. **B191** (1987) 442; Erratum-ibid. **B448** (1999) 320..

[23] J. Kalinowski *et al.*, Z. Phys. **C74** (1997) 595.

[24] H1 Collab., C. Adloff *et al.*, Phys. Lett. **B523** (2001) 234.

[25] ZEUS Collaboration; J. Breitweg *et al.*, Phys. Rev. **D63** (2001) 052002.

[26] CDF Collab., F. Abe *et al.*, Phys. Rev. Lett. **79** (1997) 4327;
DØ Collab., B. Abbott *et al.*, Phys. Rev. Lett. **80** (1998) 2051.

[27] N. Arkani-Hamed, S. Dimopoulos and G. Dvali, Phys. Lett. **B429** (1998) 263.

[28] I. Antoniadis, N. Arkani-Hamed, S. Dimopoulos and G. Dvali, Phys. Lett. **B436** (1998) 257.

[29] N. Arkani-Hamed, S. Dimopoulos and G. Dvali, Phys. Rev. **D59** (1999) 086004.

[30] J. Hewett, Phys. Rev. Lett. **82** (1999) 4765.

[31] T. Rizzo, Phys. Rev. **D59** (1999) 115010.

[32] G. Giudice, R. Rattazi and J. Wells, Nucl. Phys. **B544** (1999) 3.

[33] T. Han, J.D. Lykken and R-J. Zhang, Phys. Rev. **D59** (1999) 105006.

[34] S. Nussinov and R. Shrock, Phys. Rev. **D59** (1999) 105002.

[35] D. Bourilkov, J. High Energy Phys. **08** (1999) 006.

[36] D. Bourilkov, Phys. Rev. **D62** (2000) 076005.

[37] D. Bourilkov, Phys. Rev. **D64** (2001) 071701.